

ADAPTIVE FINITE ELEMENT ANALYSIS OF A PLATE WITH A CRACK

by

RAJEEV DUBEY

ME

1993

M

DUB

ADA

TH
ME/1993/11
D 8512



DEPARTMENT OF MECHANICAL ENGINEERING

INDIAN INSTITUTE OF TECHNOLOGY, KANPUR

JULY, 1993

ADAPTIVE FINITE ELEMENT ANALYSIS A PLATE WITH A CRACK

*A Thesis Submitted
in Partial Fulfilment of the Requirements
for the Degree of*
MASTER OF TECHNOLOGY

by
RAJEEV DUBEY

to the

**DEPARTMENT OF MECHANICAL ENGINEERING
INDIAN INSTITUTE OF TECHNOLOGY, KANPUR
JULY, 1993**

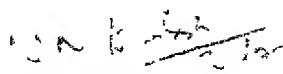
Inv. No. A. 892977

Doc No. A116269

CERTIFICATE

112

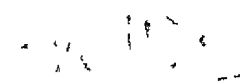
It is certified that the work contained in the thesis entitled "Adaptive Finite Element Analysis of a Plate with a Crack", by Mr. Rajeev Dubey, has been carried out under our supervision and that this work has not been submitted elsewhere for a degree.



Dr. N. N. Kishore

Mech. Engg. Department

I. I. T. Kanpur



Dr. R. Sethuraman

Mech. Engg. Department

I. I. T. Kanpur

July, 1993

ACKNOWLEDGEMENTS

I express my deep sense of indebtedness and gratitude to Dr. N.N. Kishore and Dr. R. Sethuraman for their guidance, encouragement and criticism at all stages of this work.

I will always cherish the fruitful company of dear friends Anirvan, Arun, Krishna Mohan ji, Manmohan ji, Mutul, Navaneeth, Samudra, Shaligram. Shelhar and Upendra who stood by at needful hours as well as made my stay at IITK pleasant.

JULY, 1993

RAJEEV DUBEY

H O P E

CONTENTS

	LIST OF FIGURES	vi
	NOTATIONS	ix
	ABSTRACT	xi
CHAPTER I	INTRODUCTION	
	1.1 A Brief Discussion on Bending of Plates	1
	1.2 Literature Survey	3
	1.2.1 Plate Bending	3
	1.2.2 Plates with crack	5
	1.2.3 Adaptive Analysis	7
	1.3 Present Work	8
CHAPTER II	PLATE BENDING FORMULATION	
	2.1 The Reissner-Mindlin Plate Formulation	10
	2.2 The Mixed Finite Element Formulation and its Stability	17
	2.3 The Choice of Triangular Elements: A Discussion	21
CHAPTER III	ADAPTIVE REFINEMENT FOR PLATE BENDING PROBLEMS	
	3.1 Evaluation of Energy Norm for Plate Bending Problems	26
	3.2 Superconvergent Recovery Procedures	26
	3.3 Discrete Superconvergent Recovery in an Element Pattern	28
	3.4 Automatic Mesh Refinement	36
	3.5 Algorithm for Adaptive Mesh Refinement	39
CHAPTER IV	RESULTS AND DISCUSSION	
	4.1 Plate with no Crack	41
	4.2 Plate with no Crack	42
CHAPTER V	CONCLUSIONS AND SCOPE FOR FURTHER WORK	
	5.1 Conclusions	66
	5.2 Scope for Further Work	66
	REFERENCES	68

LIST OF FIGURES

2.1	General Case of a Plate Subjected to Lateral Loading	11
2.2	Element Patch Tests on T 6/3	19
2.3	Element Patch Tests on T 6/3 P 3	20
3.1	Patch Fitting	27
3.2	Typical Element Patches in One Dimension Showing the Least Square Fit to Sample Superconvergent Gauss Point Values	30
3.3	Computation of Superconvergent Nodal Values for Linear and Quadratic Quadrilateral Elements	31
3.4	Computation of Superconvergent Nodal Values for Linear and Quadratic Triangular Elements	34
3.5	Some Element Subdivision Methods	37
3.6	Element Subdivision Method Used in the Present Work	38
4.1a	A Square Plate with all Edges Fixed and Subjected to Uniformly Distributed Lateral Loading	44
4.1b	Symmetric Quarter of the Plate for the Case Shown in Fig. 4.1a	44
4.2	Mesh configurations at Different Stages of Adaptive Mesh Refinement for the Symmetric Quarter in Fig. 4.1b	45
4.3	Variation of Lateral Displacement w along Center Line Parallel to X-Axis at Different Stages of Mesh Refinement for the Symmetric	

4.4	Variation of Lateral Displacement w along Center Line Parallel to Y-Axis at Different Stages of Mesh Refinement for the Symmetric Quarter in Fig. 4.1b	47
4.5	Variation of Moment M_x along Center Line Parallel to X-Axis at Different Stages of Mesh Refinement for the Symmetric Quarter in Fig. 4.1b	48
4.6	Variation of Moment M_y along Center Line Parallel to Y-Axis at Different Stages of Mesh Refinement for the Symmetric Quarter in Fig. 4.1b	49
4.7a	A Square Plate with a Central Crack subjected to Uniformly Distributed Bending Moment at the Two Edges Parallel to the Crack and the Remaining Two Edges Free	50
4.7b	Symmetric Quarter of the Plate for the Case Shown in Fig. 4.7a	50
4.8	Starting Mesh Configuration for the Symmetric Quarter Shown in Fig. 4.7b	51
4.9	Variation of Moment M_y (FE Values and Analytical Values) along the Center Line Parallel to X-Axis for the Case Shown in Fig. 4.7b	52
4.10a	A Square Plate with a Central Crack Subjected to Uniformly Distributed Loading, two Edges Parallel to the Crack Fixed and the Remaining Two Edges Free	53
4.10b	Symmetric Quarter of the Plate for the Case	

4.11	Starting Mesh Configuration for the Symmetric Quarter Shown in Fig. 4.10b	54
4.12	Mesh configurations at different stages of Adaptive Mesh Refinement for the Symmetric Quarter in Fig. 4.10b	55
4.13	Variation of Lateral Displacement w along Center Line Parallel to X-Axis at Different Stages of Mesh Refinement for the Symmetric Quarter in Fig. 4.10b	60
4.14	Variation of Moment M_y along Center Line Parallel to X-Axis at Different Stages of Mesh Refinement for the Symmetric Quarter in Fig. 4.10b	61
4.15	Variation of Maximum Energy Norm Error with Global Number of Degrees of Freedom for the Symmetric Quarter of the Plate Shown in Fig. 4.10b	62
4.16	Variation of Crack Tip Moment M_y with respect to Different Stages of Mesh Refinement for Fig. 4.10b	63

NOTATIONS

A	Part of Element Stiffness Matrix
a	Coefficient Matrix
a	Half Crack Length
B	Part of Element Stiffness Matrix
C	Part of Element Stiffness Matrix
D	Property Matrix
E	Modulus of Elasticity
e	Error
f	Load Vector
G	Shear Modulus of Elasticity
h	Size of Subdivision
L	Differential Operator
M,M	Moment
N,N	Shape function
n	Number of Variables, Constant
P	Part of Element Stiffness Matrix
p	Order of Polynomial
q	Uniformly Distributed Load
S	Shear Force
T,T	Edge Moment
t	Thickness
u	Displacement along x
v	Displacement along y
w	Displacement along z
x	Cartesian Coordinate, Distance

y	Cartesian Coordinate Distance
z	Cartesian Coordinate, Distance
Γ	Boundary
γ	Shear Strain
δ	Constant
ϵ	Strain
θ	Rotation
ν	Poisson's Ratio
Σ	Summation
σ	Stress
τ	Shear Stress
Ω	Area

ABSTRACT

The plate bending problems involving cracks have a wide range of practical applications. The finite element method with adaptive mesh refinement such that local mesh refinement takes place in the zones of very high stress gradient gives optimum mesh refinement to the solution of such problems. A posteriori error estimation and an automatic mesh refinement strategy play vital roles in developing fully automatic adaptive analysis procedures. A posteriori error estimate is used in the adaptive procedure to assess the reliability of the finite element approximation and to guide adaptive refinement. Coupled with superconvergent patch recovery technique, the adaptive analysis becomes a very powerful tool for the solution of a wide range of complex plate bending problems.

The other important aspect of plate bending problems is their finite element formulation such that thick as well as thin plates can be accommodated in a single formulation. The Reissner Mindlin theory for the analysis of plate bending problems when cast with mixed formulation in finite element method allows to explore the possibility of developing special plate bending elements called 'robust elements' which would work for thick plates as well as in the limiting case of thin plate theory. The major difficulty in designing such elements was the satisfaction of Babuska-Brezzi stability requirements. A much simpler way which can be applied in terms of very simple algebraic equations exists via the medium of patch test which is (nearly) always also

sufficient

A robust triangular element which satisfies all the above requirements has been used in the present work. An efficient finite element code has been developed which requires a minimal information from the user. It is seen that the element works satisfactorily and the critical zones in plate bending cases which include fixed edges of a plate, crack tip zone etc. are successively more refined. Due to the readjustment of the node positions, though not monotonically, the solutions tend to expected values in a few steps.

INTRODUCTION

Plates with lateral loads find numerous applications in engineering. The common examples being army tank bodies under various types of loadings, aero structures, offshore platforms, navy ship bodies, etc. The presence of cracks in plate structures under such crucial applications makes the stress analysis of such bodies very important. But it is observed that starting from plates without cracks to plates with cracks, the plate bending problems rarely yield to closed form solutions. This necessitates the use of numerical methods. For plates with cracks the crack tips carry very high stresses. Finite element method offers itself as a very suitable method for all such problems. Once the problem is formulated for finite element analysis, it becomes necessary to enquire about the accuracy of the results. Also, in the regions of high stresses which frequently occur in the plates with cracks, the mesh refinement to approximate the exact solution in an optimum way becomes very important. For this the adaptive mesh refinement procedures are used where the magnitude of the error (of the desired quantity) guides the further refinement of the finite element mesh.

1.1 A BRIEF DISCUSSION ON BENDING OF PLATES

The bending properties of plate depend greatly on its thickness as compared with its other dimensions. A comprehensive

review can be found in the book by Timoshenko et al [1959]

If lateral deflection of a plate is small in comparison with its thickness, a very satisfactory approximate theory of bending of plates is developed which is called thin plate theory. All stress components can be expressed by deflection (say w) of the plate, which is a function of the two coordinates in the plane of the plate. This function has to satisfy a linear partial differential equation, which, together with boundary conditions, completely defines w . Thus the solution of this equation gives all necessary information for calculating stresses at any point of the plate.

Thick plate theory considers plates as a three dimensional problem of elasticity. Here, in addition to mid plane deflections $w(x,y)$, it is also necessary to consider shear deformations θ_x, θ_y and shear force components S_x, S_y in the x - y plane.

In the present work based on FEM analysis a 'robust' triangular plate bending element is used. The element is based on independent interpolations for slopes, displacements, and shear forces. The name robust means that the element used in the formulation works in the case of thick plates as well as in the limiting case of thin plates.

Once the finite element results are obtained, an obvious question arises about their accuracy. For this reason the subject

of error estimates for finite element solutions and a consequent adaptive analysis in which the approximation is successively refined to achieve predetermined standards of accuracy is central to the effective use of practical, engineering, analysis.

The present work uses a simple error estimator coupled with an automatic mesh generator (limited to rectangular domains).

Two methods of refining a finite element solution exist. The first is the simple reduction of the subdivision size which may be local or global (h-refinement). The second refinement process increases the order of the polynomial trial function approximation in a predefined element subdivision (p-refinement). Here the first method is used. The reason for this choice being its simplicity and also the fact that for plate bending problems it is very difficult to find out higher order elements that pass through the convergence requirements successfully.

1.2 LITERATURE SURVEY

1.2.1 PLATE BENDING :

The deformation of a thin plate element is completely described by its lateral displacement, $w(x,y)$. As the governing differential equation is of fourth order which becomes a second order equation in the weak formulation, an acceptable element must display C^1 continuity in the limit of mesh refinement. This means that w and its first derivatives must be continuous across interelement boundaries. But the formulation of C^1 element being

very difficult an alternative was introduced in late sixties and treats plates as a degenerate case of a three dimensional approximation with a simplified strain distribution in the thickness direction [Ahamed et al., 1968, 1969].

It was realised that the reduction of shear terms should permit the return to thin plate theory. Here, however, difficulties have been encountered such as 'locking' (i.e. the reduction of displacements to zero) or singular mechanisms of the elements [Pugh et al., 1978; Hinton et al., 1979]. To eliminate locking, 'reduced integration' concepts were introduced [Pawsey et al., 1971; Zienkiewicz et al., 1971].

On finding that reduced integration concepts were only partly successful, much research work followed the realization that the approximation involved was identical to that used by Reissner and Mindlin and that the problem could be cast as a mixed formulation involving rotations of the normal (θ), shear forces (S), and lateral displacements (w) as the primary variables [Lee et al., 1982]. Again it was observed that no efficient element could be developed on the basis of mixed formulation alone [Zienkiewicz et al., 1988].

Perhaps the main difficulty stemmed from the fact that applying the Babuska-Brezzi stability requirements necessary for all mixed formulations and thus designing suitable elements becomes very difficult [Zienkiewicz et al., 1988].

A much simpler set of necessary requirements was devised for mixed formulation via the medium of patch test and it was shown [Zienkiewicz et al., 1986] that it was (nearly) always also sufficient for ensuring stability (and hence absence of both locking and singularity). The general algebraic conditions of Babuska and Brezzi were given a simpler form and a conceptual application of the patch tests serves to point out the instability of several well known formulations.

In the year 1988 a new triangular plate bending element was presented. This element is based on independent interpolations for slopes, displacements and shear forces and it is shown that it does not suffer from any defect common to other Mindlin plate elements. The element is robust and therefore suitable for use in commercial codes without restrictive caveats [Zienkiewicz et al., 1988].

1.2.2 PLATES WITH CRACK

It was only after the year 1960 that the stress problem of cracked plates was examined from a higher order plate bending theory taking shear deformation into account. The earliest attempt [Knowles et al., 1960] was concerned with the problem of an infinite plate under uniform uniaxial bending far from the crack and was restricted to the case of vanishingly small plate thickness. The same problem was studied considering the plate thickness to be finite [Hartranft et al., 1968]. All the cases in

these investigations were based on Reissner's theory and led to the conclusion that singular stresses under bending have the same functional form as in the plane stress case [Williams et al., 1957]. The predictions of classical theory [Williams et al., 1961] are known to be erroneous with respect to the angular distribution of stress around the crack tip. As a more serious practical consequence there is an associated error in predicting the stress intensity factor whose importance in fracture mechanics is well known. Results reported [Hartranft et al., 1968; Wang et al., 1968] show that the stress intensity factor varies very rapidly in the h/a range of 0.0 to 0.25. In fact it was shown that the stress intensity factor versus h/a curve has infinite slope at h/a equal to zero [Hartranft et al., 1968]. It is seen that even for h/a ratio as small as 0.2 the bending stress intensity factor is 62% greater than that given earlier [Knowles et al., 1960] for h/a tending to zero. Since h/a does not appear as a parameter in classical theory formulation, the inadequacy of this theory in handling the bending case in crack problems becomes apparent. In another paper [Murthy et al., 1981] the finiteness of the plate was taken into account and the analysis here was based on differential approach. Shear deformation was taken into account through the use of Reissner's theory. No restriction was put on the h/a ratio so that the thickness effect could automatically be taken into account.

1.2 3 ADAPTIVE ANALYSIS

The subject of error estimates for finite element solutions and a consequent adaptive analysis in which the approximation is successively refined to achieve predetermined standards of accuracy, is central to the effective use of finite element codes for practical, engineering analysis. Much of the pioneering mathematical work [Babuska et al., 1978, 1979; Babuska, Peano et al., 1978; Craig et al., 1986; Kelly et al., 1983; Gago et al., 1983] needs to be translated to engineering usage. The two main problems encountered have been [Zienkiewicz et al., 1987]

1. The cost of computations associated with error estimation and the difficulty of implementing such computations into an existing code structure.
2. The virtual impossibility of embracing a fully adaptive structure into an existing code structure.

The year 1987 saw a new error estimator by Zienkiewicz-Zhu [Zienkiewicz et al., 1987]. This estimator allows the global energy norm to be well estimated and also gives a good evaluation of local errors. It can be combined with a full adaptive process of refinement or, more simply provide guidance for mesh redesign which allows the user to obtain a desired accuracy.

In a later work the Zienkiewicz-Zhu error estimator was shown to be effective in problems of plate flexure. When used in conjunction with triangular elements and an adaptive mesh

generator allowing a prescribed size of elements to be developed very fast adaptive convergence for results of specified accuracy is achieved [Zienkiewicz et al., 1989].

In another work, presented in two parts [Zienkiewicz et al., 1992], the issue of posteriori error estimation was discussed. A general recovery technique is developed for determining the derivatives (stresses) of the finite element solutions at the nodes. The implementation of recovery technique is simple and cost effective. The recovered nodal values of the derivatives with linear and cubic elements are superconvergent. One order higher accuracy is achieved by the procedure with linear and cubic elements but two order higher accuracy is achieved for the derivatives with quadratic elements.

In second part of the paper a theorem is derived showing the dependence of effectivity index for the Zienkiewicz-Zhu error estimator on the convergence rate of the recovered solution. This shows that with superconvergent recovery the effectivity index tends asymptotically to unity. The superconvergent recovery technique developed in the first part of the paper is used in the computation of the Zienkiewicz-Zhu error estimator to demonstrate accurate estimation of the exact error attainable.

1.3 PRESENT WORK

Present work is an attempt to integrate the FEM analysis of bending of plates with cracks and adaptive mesh refinement. An

efficient element (robust triangular element) has been made use of to solve the thin as well as thick plate problems. Also Zienkiewicz-Zhu error estimator is used for the refinement procedure to automatically refine the mesh wherever the error is large.

Thus, in the present thesis, chapter II describes the basics of plate bending and finite element formulation and chapter III describes the adaptive mesh refinement procedure for plate bending problems. Chapter IV presents results of some typical problems and discusses their validity. Chapter V summarizes the conclusions and delineates the scope for further study.

PLATE BENDING FORMULATION

2.1 THE REISSNER-MINDLIN PLATE FORMULATION

Fig. 2.1 shows a general case of plate subjected to lateral loading. The x and y coordinate- are defined to be in the mid plane of the plate and the z coordinate in normal direction with corresponding component displacements u , v , w . The following assumptions are made to simplify the analysis :

- (a) The strains and stresses in the z -direction are neglected i.e., ($\epsilon_z = 0$, and $\sigma_z = 0$).
- (b) The normals to the middle plane of the plate remain straight during deformation.

Using the above assumptions all the displacements can be written in terms of mid-plane rotations θ_x , θ_y and lateral displacement w of the mid plane.

Thus,

$$u = z.\theta_x \quad \text{and} \quad v = z.\theta_y \quad (2.1)$$

where z is measured from the middle plane and the corresponding strains are given as

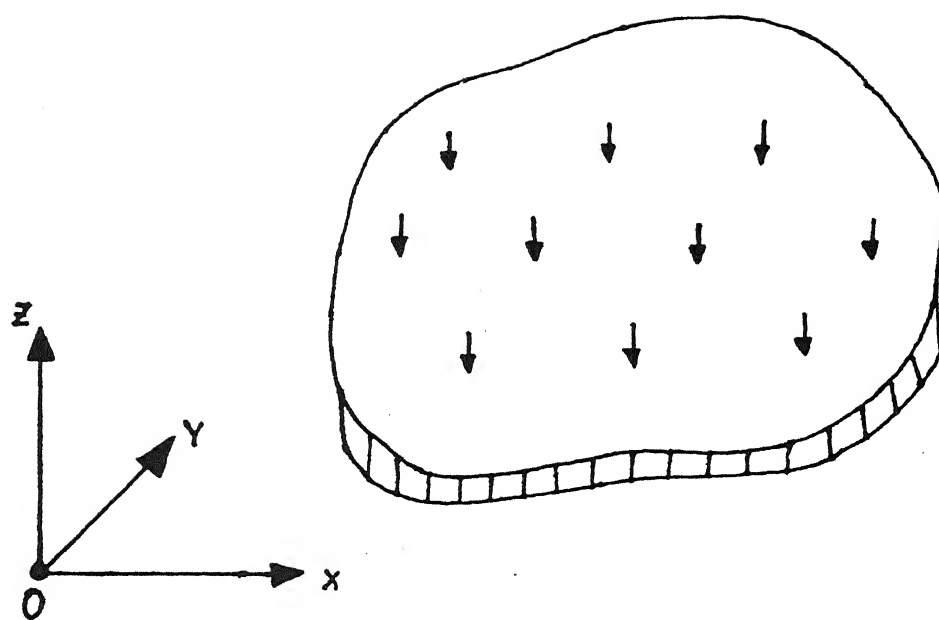


Figure 2.1 General Case of a Plate Subjected to Lateral Loading

$$= z. \partial \theta_x / \partial x,$$

$$= z. \partial \theta_y / \partial y$$

$$y + \partial v / \partial x,$$

$$+ \partial w / \partial v = \theta_x + \partial w / \partial x,$$

$$+ \partial w / \partial y = \theta_y + \partial w / \partial y$$

be written in matrix form as,

$$\begin{Bmatrix} \epsilon_x \\ \epsilon_y \\ \gamma_{xy} \end{Bmatrix} = \begin{bmatrix} \partial/\partial x & 0 \\ 0 & \partial/\partial y \\ \partial/\partial y & \partial/\partial x \end{bmatrix} \begin{Bmatrix} u \\ v \end{Bmatrix} =$$

$$\begin{Bmatrix} \epsilon_x \\ \epsilon_y \\ \gamma_{xy} \end{Bmatrix} = \begin{Bmatrix} \theta_x \\ \theta_y \end{Bmatrix} + \begin{Bmatrix} \partial w / \partial x \\ \partial w / \partial y \end{Bmatrix}$$

esses can be written as,

$$\begin{Bmatrix} \sigma_x \\ \sigma_y \\ \tau_{xy} \end{Bmatrix} = \frac{E t^3}{12(1-\nu^2)} \begin{bmatrix} 1 & \nu & 0 \\ \nu & 1 & 0 \\ 0 & 0 & (1-\nu)/2 \end{bmatrix}$$

....

$$\text{or } \bar{\sigma} = D\bar{\epsilon}$$

and

$$\begin{Bmatrix} \tau_{xz} \\ \tau_{yz} \end{Bmatrix} = \begin{bmatrix} G & 0 \\ 0 & G \end{bmatrix} \begin{Bmatrix} \gamma_{xz} \\ \gamma_{yz} \end{Bmatrix} \quad (2.2c)$$

Introducing linear elastic relations and integrating stresses in the thickness direction permits stress resultants to be determined in terms of mid plane rotations and displacements. Assuming isotropic behaviour (with constant E and ν) in the x-y plane, with the lateral shear behaviour independently defined by a shear modulus G.

If the stress resultant moments are defined as

$$\begin{aligned} M_x &= \int_{-l/2}^{l/2} \sigma_x z \, dz \\ M_y &= \int_{-l/2}^{l/2} \sigma_y z \, dz \\ M_{xy} &= \int_{-l/2}^{l/2} \sigma_{xy} z \, dz \end{aligned} \quad (2.3)$$

or, in the matrix form,

$$\mathbf{M}^T = \begin{bmatrix} M_x & M_y & M_{xy} \end{bmatrix}$$

these can be written as

$$\mathbf{M} = \mathbf{DL}\theta \quad (2.4)$$

where

$$\begin{bmatrix} \theta_x & \theta_y \end{bmatrix}$$

$$\frac{t^a}{(1-\nu^2)} \begin{bmatrix} 1 & \nu & 0 \\ \nu & 1 & 0 \\ 0 & 0 & (1-\nu)/2 \end{bmatrix}$$

$$\begin{bmatrix} \partial/\partial x & 0 \\ 0 & \partial/\partial y \\ \partial/\partial y & \partial/\partial x \end{bmatrix}$$

.....(2.5)

shear resultant can be evaluated similarly as

$$S_x = \int_{-l/2}^{l/2} \tau_{xz} dz \quad ,$$

(2.6)

$$S_y = \int_{-l/2}^{l/2} \tau_{yz} dz \quad ,$$

the matrix form

$$S^T = [S_x \ S_y]$$

more convenient to define global shear strains in terms of stress resultants and then

$$\begin{bmatrix} \theta_x + \partial w / \partial x \\ \theta_y + \partial w / \partial y \end{bmatrix} = \theta + \nabla w = cS \quad (2.7)$$

where

$$c = \frac{\delta}{Gt} \begin{bmatrix} 1 & 0 \\ 0 & 1 \end{bmatrix} \quad (2.8)$$

The parameter δ is equal to unity in the present derivation but is conveniently taken as a value of 6/5 [Zienkiewicz et al. 1988] to account for non-uniform shear stress distribution.

The full statement of the problem involves the well known equilibrium resultant equations. For moment shear equilibrium,

$$L^T M + S = L^T D L \theta + S = 0 \quad (2.9)$$

and for lateral equilibrium,

$$\nabla^T S + q = 0 \quad (2.10)$$

q being the applied load intensity normal to the plate rotation.

The three sets of equations (2.9), (2.7), and (2.10) define the plate bending problem in its generality in terms of three sets of variables θ , S , and w when appropriate boundary conditions are imposed.

Indeed, the Kirchhoff thin plate bending theory is also available by imposing an infinite shear modulus G or putting $c=0$. It is easy to see that in this limiting case both S and θ can be eliminated by applying the operator ∇^T to Eq.(2.9) and

substituting Eqs 2.7 and 2.10 This gives the well known biharmonic thin plate equation

$$(\nabla^T L^T D L \nabla) w + q = 0 \quad (2.11)$$

As it is clear that closed form solution of the above formulations is rarely possible, numerical methods are adopted. In Finite Element Method it is known that for any type of element being used, the convergence requirements must be satisfied. Convergence requirements are conditions that guarantee that exact solutions will be approached as more and more elements are used to model the structure. These requirements are listed below.

1. The displacement field within an element must be continuous.
2. The element must be able to assume a state of constant strain.

In the limit of mesh refinement but not necessarily in larger elements

3. Rigid body modes must be present.
4. Elements must be compatible.

The convergence requirement No. 4. says that Eq. (2.11) requires C^1 continuity. As formulation of C^1 element is very difficult in this case, mixed formulation is adopted.

With finite values of shear flexibility κ it is easy to eliminate the variables S and use for solution only the θ and w

variables. This indeed corresponds to the usual formulation of the problem in approximate form for which such devices as reduced integration had to be introduced to allow approximation to proceed towards thin, Kirchhoff limit. In what follows a full mixed form with three variables will be used, which should yield solution for both thick plates and the limiting thin plate situation.

2.2 THE MIXED FINITE ELEMENT FORMULATION AND ITS STABILITY

[Zienkiewicz et al., 1988]

The Finite Element formulation of the mixed problem follows standard procedure. The problem is formulated in the three sets of unknowns θ , S , and w which are approximated by appropriate shape functions and parameters as

$$\begin{aligned}\theta &= N_{\theta} \bar{\theta} \\ S &= N_S \bar{S} \\ w &= N_w \bar{w}\end{aligned}\tag{2.12}$$

where N_{θ} , N_S and N_w are shape functions and $\bar{\theta}$, \bar{S} , and \bar{w} are nodal variables.

Now using Galerkin method with weighting functions N_{θ}^T , N_S^T , N_w^T in the weak form on equations (2.9), (2.7) and (2.10) respectively (using Gauss integrals on the first and last equations) the following equations are obtained

$$\begin{bmatrix} A & B & 0 \\ B^T & P & C \\ 0 & C^T & 0 \end{bmatrix} \begin{Bmatrix} \bar{\theta} \\ \bar{S} \\ \bar{w} \end{Bmatrix} = \begin{Bmatrix} f_1 \\ f_2 \\ f_3 \end{Bmatrix} \quad (2.13)$$

In the above

$$\begin{aligned} A &= \int_{\Omega} (LN_{\theta})^T D (LN_{\theta}) d\Omega \\ B &= -\int_{\Omega} LN_{\theta}^T N_s d\Omega \\ C &= -\int_{\Omega} N_s^T \nabla N_v d\Omega \end{aligned} \quad (2.14)$$

$$f_1 = \int_{\Gamma_t} N_{\theta}^T T d\Gamma$$

$$f_2 = 0$$

$$f_3 = -\int_{\Gamma_t} N_v^T F d\Gamma - \int_{\Omega} N_v^T q d\Omega$$

and

$$P = \int_{\Omega} N_s^T c N_s d\Omega$$

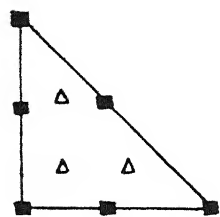
is a term which becomes zero in Kirchhoff thin plate theory.

In the above T represents the two moment components imposed on the boundary by the traction and F the imposed shear force. The shape functions N_{θ} and N_v are conveniently chosen to have C^1 continuity but N_s can be discontinuous between elements.

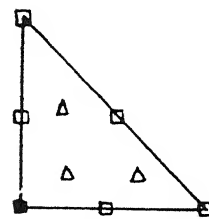
CONSTRAINED TEST

RELAXED TEST

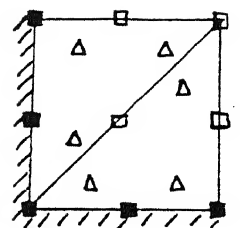
INFINITE TEST



$$\begin{aligned} n_{\theta} &= 0 \\ n_s &= 6 \\ n_w &= 0 \\ \alpha &= 0 \quad \beta = \infty \end{aligned}$$



$$\begin{aligned} n_{\theta} &= 10 \\ n_s &= 6 \\ n_w &= 5 \\ \alpha &= 15 / 6 \quad \beta = 6 / 5 \end{aligned}$$

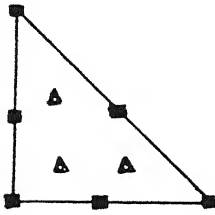


$$\begin{aligned} n_{\theta} &= 8 \\ n_s &= 12 \\ n_w &= 4 \\ \alpha &= 1 \quad \beta = 3 \end{aligned}$$

$\square \blacksquare$	θ, w	2, 1	D.O.F. PER NODE (SOLID SHADE FOR RESTRAINTS)
$\triangle \blacktriangle$	s	2	D.O.F. PER NODE (SOLID SHADE FOR RESTRAINTS)
$\circ \bullet$	θ	2	D.O.F. PER NODE (SOLID SHADE FOR RESTRAINTS)

Figure 2.2 Element Patch Tests on T 6/3 $\alpha = (n_{\theta} + n_w) / n_s$, $\beta = n_s / n_w$

CONSTRAINED TEST



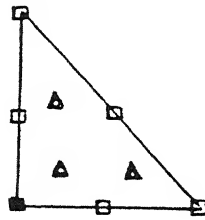
$$n_e = 6$$

$$n_s = 6$$

$$n_w = 0$$

$$\alpha = 1 \quad \beta = \infty$$

RELAXED TEST



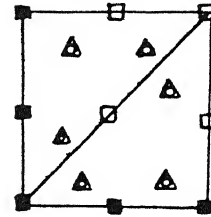
$$n_e = 16$$

$$n_s = 6$$

$$n_w = 5$$

$$\alpha = 21 / 6 \quad \beta = 6 / 5$$

INFINITE TEST



$$n_e = 20$$

$$n_s = 12$$

$$n_w = 4$$

$$\alpha = 2 \quad \beta = 3$$

Figure 2.3 Element Patch Tests on T 6/3 B 3 $\alpha = (n_e + n_w) / n_s$, $\beta = n_s /$

Indeed, such choice allows \bar{S} to be eliminated at element level when $P \neq 0$ and the main problem includes only the variables $\bar{\theta}$ and \bar{w} .

The choice of the shape function and variables needs, however, to be such that the Babuska-Brezzi conditions are satisfied by the system and stability is ensured. The most vital and strictly necessary condition for non-singularity of the equation system (2.13) is that

$$\alpha = \frac{n_{\theta} + n_w}{n_s} \geq 1 \quad (2.15)$$

and

$$\beta = \frac{n_s}{n_w} \geq 1,$$

where n_{θ} , n_s and n_w stand for the number of variables $\bar{\theta}$, \bar{S} , \bar{w} respectively in any single element, element patch or indeed the whole problem. If either condition is violated mechanisms or locking behaviour are obtained.

2.3 THE CHOICE OF TRIANGULAR ELEMENTS: A DISCUSSION

[Zienkiewicz et al., 1988]

It is well known that any complex geometric domain can be discretized into triangular elements. Also from the point of view of further mesh refinement, the triangular elements can be subdivided very conveniently. In the mixed finite element formulation the simplest quadratic Triangle is one in which six boundary nodes are used to determine a quadratic variation of θ and w , and the shear resultants S are determined with no element

interconnection by a linear field defined by three internal nodes. This possible element is termed T6/3 and in Fig. 2.2 its behaviour is illustrated in single element constrained and relaxed patch tests as well as in an infinite patch. In the relaxed test only the minimum number of degrees of freedom on the boundaries of the element (i.e. 3) are prescribed and condition (2.15) is satisfied.

The infinite test is done with the assumption that two elements are added to a region in which all values are prescribed. The performance at this test determines in general the quality of element behaviour, depending on the values of α and β achieved (though of course they still have to obey Eq. (2.15)). In this particular example $\alpha=1$, indicating an incipient locking possibility. It is evident from the above that T6/3 is not a satisfactory element, but examination of the results indicates that satisfaction of the requirements could be achieved by addition of θ variables in the interior of the element. This is accounted by creating three internal nodes or bubble functions, giving element T6/3 B3. The functions used here are quartics of the form $L_1^2 L_2 L_3$, etc.

Fig. 2.3 repeats the three tests on this element, which in all cases passes successfully.

Thus in the following finite element analysis mixed formulation with $\theta_x, \theta_y, w, S_x$ and S_y as variables is chosen. The element adopted is T6/3 B3 which has six nodes on its edges and three internal nodes. The element stiffness matrix is a matrix of

the order of 30×30 .

Now with this element being used for the plate bending problems, it is an obvious question as to what extent the analysis is correct for the stress concentration zones. For this to be answered, adaptive analysis comes in the picture. The following chapter deals with this aspect of the problem and gives an implementation algorithm.

CHAPTER III

ADAPTIVE REFINEMENT FOR PLATE BENDING PROBLEMS

The finite element method offers a numerically approximate solution of a mathematically posed problem. The differences between the exact and approximate solution, e.g., errors in displacements [Zienkiewicz, Taylor, 1989]

$$e_u = u - \hat{u}$$

and the errors in stresses

$$e_\sigma = \sigma - \hat{\sigma}$$

where u , σ refer to exact displacement and stress solutions and \hat{u} , $\hat{\sigma}$ refer to approximate solutions respectively, decrease as the size of subdivision 'h' gets smaller or as 'p', the order of the polynomial in the trial function used increases. This establishes convergence and the acceptability of the various finite element forms.

This chapter has the following objectives :

- (a) Determine the error that has occurred in a particular finite element analysis (a posteriori error estimate).
- (b) Give a procedure how best to refine the approximation to achieve results of a given desired accuracy economically.

In general the iteration between (a) and (b) is adaptive and several steps are required to achieve results that are optimal.

The exact solution to a practical problem is not available

except for some very simple cases. Thus more accurate if not exact results have to be extracted from the available finite element results.

The Zienkiewicz-Zhu error estimator [Zienkiewicz et al., 1987] has proved to be economical and effective both in evaluating errors simply for a given analysis and as a prelude to adaptive processes. The essence of the procedure is to use the difference between the post-processed, recovered, more accurate gradients (stresses) σ^* and those given directly by the finite element solutions σ_h ,

i.e.

$$e_{\sigma}^* = \sigma^* - \sigma_h \quad (3.1)$$

as a measure of the local error [Zienkiewicz et al., 1992].

The error can then be evaluated in any appropriate norm defined in terms of derivative errors. Most frequently the energy is used as it is physically more appealing, though several other norms can be adopted.

It is obvious that the success of the procedure is dependent on the accuracy of the recovered gradients. The global h_2 projection and simple averaging techniques were originally recommended by Zienkiewicz and Zhu [Zienkiewicz et al., 1987] but it was soon found that such recovery techniques were inadequate for quadratic approximations.

Recently a highly accurate recovery process was introduced by

the same authors [Zienkiewicz et al., 1992]. The process has superconvergent properties and its use in the Zienkiewicz-Zhu error estimator is highly beneficial.

3.1 EVALUATION OF ENERGY NORM FOR PLATE BENDING PROBLEMS

The problem of thick (Reissner-Mindlin) plate can be written in the general form as given by equations (2.9) and (2.10). With the constitutive relations given by equations (2.4) and (2.7) and defining α to be shear rigidity, the energy norm of the displacement or of the error can be written as

$$||e||^2 = \int_{\Omega} (\mathbf{M} - \mathbf{M}_h)^T \mathbf{D}^{-1} (\mathbf{M} - \mathbf{M}_h) d\Omega + \int_{\Omega} (\mathbf{S} - \mathbf{S}_h)^T \alpha^{-1} (\mathbf{S} - \mathbf{S}_h) d\Omega \quad (3.2)$$

Here \mathbf{M}_h and \mathbf{S}_h are the finite element approximations to the exact \mathbf{M} and \mathbf{S} . As the exact values \mathbf{M} and \mathbf{S} are not available, they have to be represented by some projected values of those obtained from the FEM solution itself giving the a posteriori error estimate [Zienkiewicz et al., 1989].

3.2 SUPERCONVERGENT RECOVERY PROCEDURES

The object of the recovery of the finite element derivatives is to find nodal parameters $\bar{\sigma}^*$ such that the smoothened continuous stress field σ^* defined by the basis functions \mathbf{N} and nodal

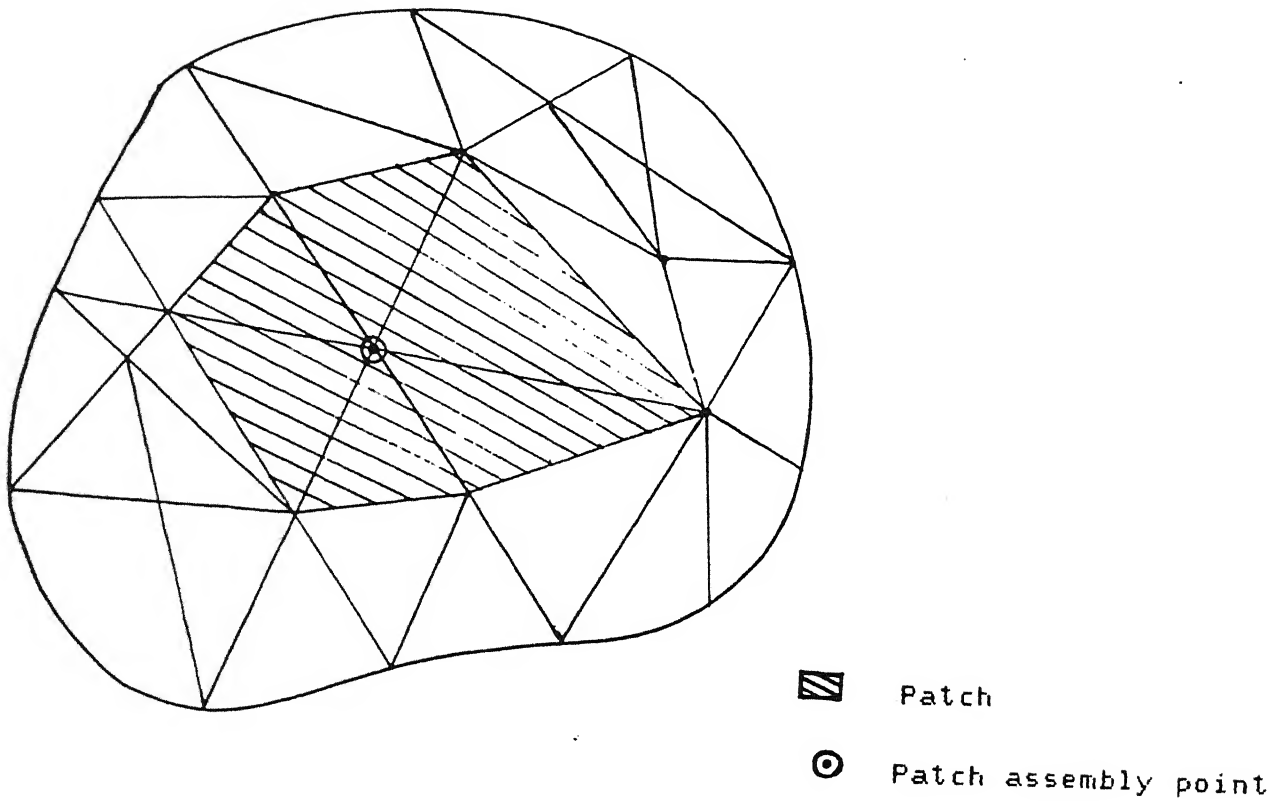


Figure 3.1 Patch Fitting

parameters $\bar{\sigma}^*$ as [Zienkiewicz et al., 1992]

$$\sigma^* = N \bar{\sigma}^* \quad (3.3)$$

is more accurate than σ_h . In the above N are the same basis functions as the ones used for the interpolation of the displacements. Here σ (with superscripts) is used as a general gradient term which may be stress, moment, etc. such that energy or its equivalent is obtained.

In the recovery process it is assumed that the nodal values $\bar{\sigma}^*$ belong to a polynomial expansion σ_p^* of the same order p as that present in the basis function N and which is valid over an element patch (the concept of patch formation is explained in Fig. (3.1) surrounding the particular assembly node considered. Such a patch represents a union of elements containing this vertex node. This polynomial expansion is used for each component of σ_p^* (or the derivatives) and

$$\sigma_p^* = P a \quad (3.4)$$

where P contains the appropriate polynomial terms and a is a set of unknown parameters. For one dimensional elements of order p , P can be written as

$$P = [1 \quad x \quad x^2 \quad \dots x^p] \quad (3.5)$$

and

$$a = [a_1 \quad a_2 \quad a_3 \quad \dots a_{p+1}] \quad (3.6)$$

In the same way writing only the complete polynomial terms, P can be written for two (or three) dimensions for the appropriate element order. Thus for two dimensions and linear expansion

$$P = [1 \quad x \quad y] \quad (3.7)$$

and for quadratic

$$P = [1 \quad x \quad y \quad x^2 \quad xy \quad y^2] \quad (3.8)$$

etc.

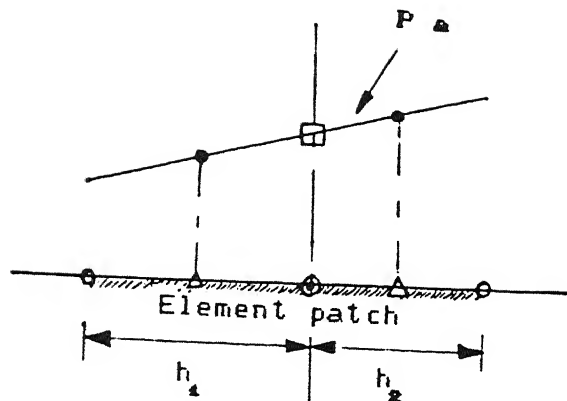
However, for quadrilaterals in which terms additional to the complete polynomial occur it appears that a slight improvement of results is obtained by using identical terms to those occurring in the shape function N . Thus for a quadrilateral

$$P = [1 \quad x \quad y \quad xy] \quad (3.9)$$

is used and similar forms for higher expansions.

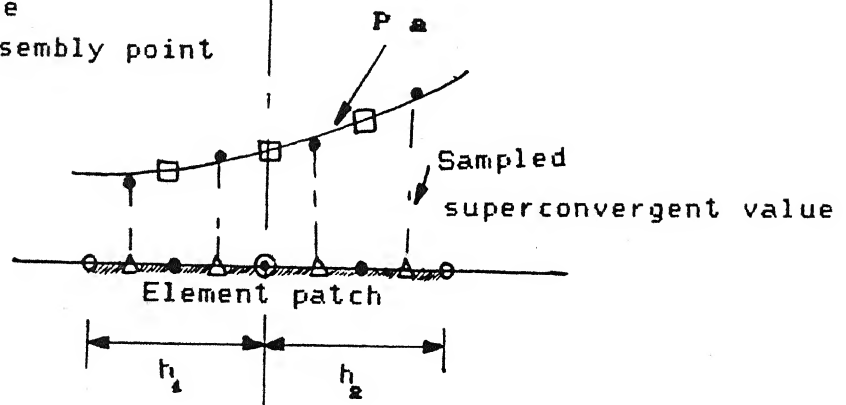
3.3 DISCRETE SUPERCONVERGENT RECOVERY IN AN ELEMENT PATCH

The determination of the unknown parameters a of the expansion given in Eq. 3.4 is made by ensuring a least square fit of this to the set of superconvergent or at least high accuracy sampling points existing in the patch considered if such points are available. To do this minimization is applied on



2 node (Linear) elements

- Δ Superconvergent Gauss point
- \square Nodal values determined by recovery procedure
- \odot Patch assembly point



3 node (Quadratic) elements

Figure 3.2 Typical Element Patches in One Dimension Showing the Least Square Fit to Sample Superconvergent Gauss Point Values

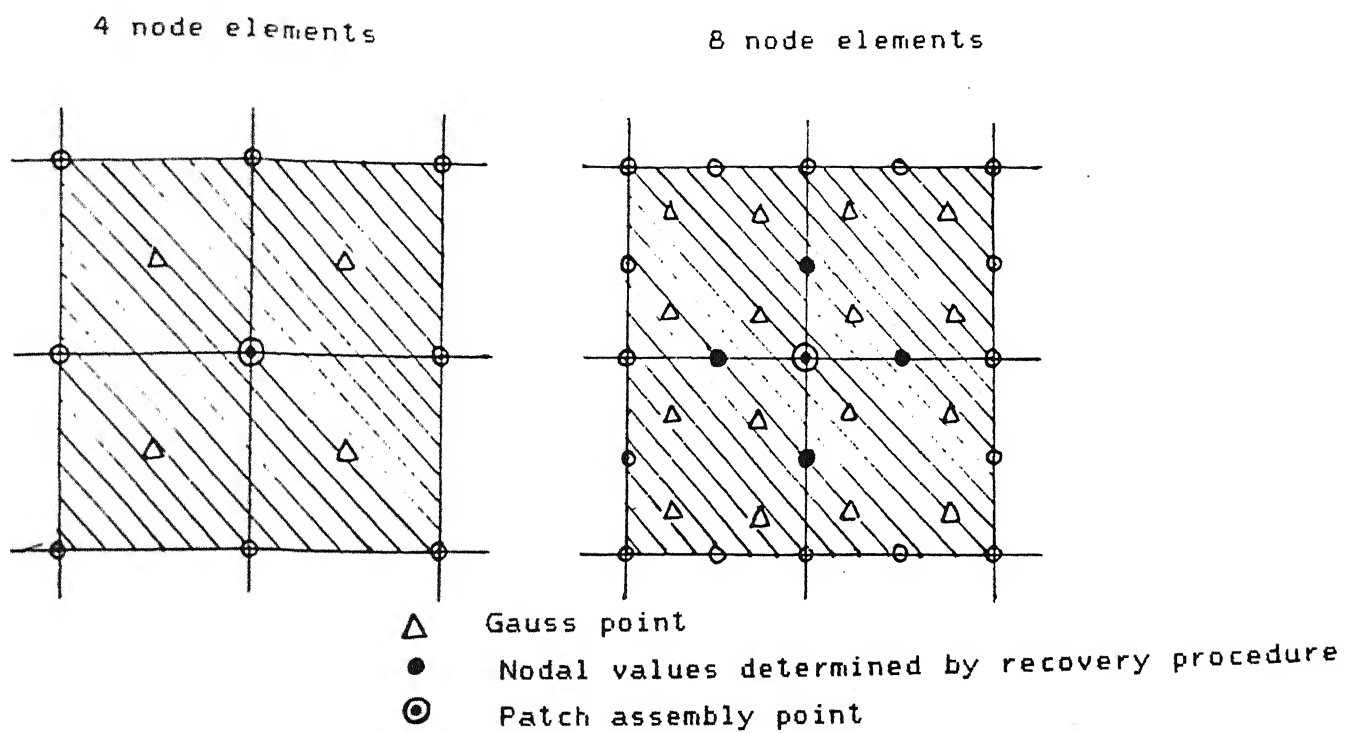


Figure 3.3 Computation of Superconvergent Nodal Values for Linear and Quadratic Quadrilateral Elements

$$\begin{aligned}
 F(\mathbf{a}) &= \sum_{i=1}^n (\sigma_h(x_i, y_i) - \sigma_p^*(x_i, y_i))^2 \\
 &= \sum_{i=1}^n (\sigma_h(x_i, y_i) - \mathbf{P}(x_i, y_i) \mathbf{a})^2
 \end{aligned} \tag{3.10}$$

where (x_i, y_i) are the coordinates of a group of sampling points, $n = mk$ is the total number of sampling points and k is the number of sampling points on each element m_j ($m_j = 1, 2, 3, \dots, m$) of the element patch [Zienkiewicz et al., 1992]. The minimization condition of $F(\mathbf{a})$ implies that \mathbf{a} satisfies

$$\sum_{i=1}^n \mathbf{P}^T(x_i, y_i) \mathbf{P}(x_i, y_i) \mathbf{a} = \sum_{i=1}^n \mathbf{P}^T(x_i, y_i) \sigma_h(x_i, y_i) \tag{3.11}$$

This can be solved in matrix form as

$$\mathbf{a} = \mathbf{A}^{-1} \mathbf{b} \tag{3.12}$$

where

$$\mathbf{A} = \sum_{i=1}^n \mathbf{P}^T(x_i, y_i) \mathbf{P}(x_i, y_i)$$

and

$$\mathbf{b} = \sum_{i=1}^n \mathbf{P}^T(x_i, y_i) \sigma_h(x_i, y_i)$$

The number of equations to be solved on each patch is modest and the recovery is performed only for each vertex node.

The procedure is therefore quite inexpensive. It is noted that precisely the same matrix \mathbf{A} occurs in the solution for each component of σ_p^* and hence only a single evaluation of this is necessary.

Once the parameters \mathbf{a} are determined the recovered nodal values of $\bar{\sigma}^*$ are calculated by insertion of appropriate coordinates into the expression for σ_p^* .

Here only the nodes inside the patch are considered. It can be expected that all values of σ_p^* in the domain of the patch are superconvergent as it fits closely to local sampling points which exhibit this property and is also of the correct polynomial order.

The procedure is explained on a one dimensional example of Fig. 3.2 where linear and quadratic elements are considered. It is well known that superconvergence of the derivatives occurs here at the Gauss points shown, and the appropriate fit of linear and quadratic polynomials over an element patch is indicated.

In Fig. 3.3 the sampling points for patches of quadrilateral elements with $p = 1$ and 2 are shown. Here again the derivatives at appropriate Gauss points are known to be superconvergent.

Obviously the procedure could be used for any order of p for such elements. In Fig. 3.4 a similar procedure is applied to triangular elements of linear and quadratic types.

For triangular shapes the existence and the locations of superconvergent points are still a matter which does not appear to have been fully explored mathematically despite the early work of Moan [Moan, 1974] suggesting the existence of optimal

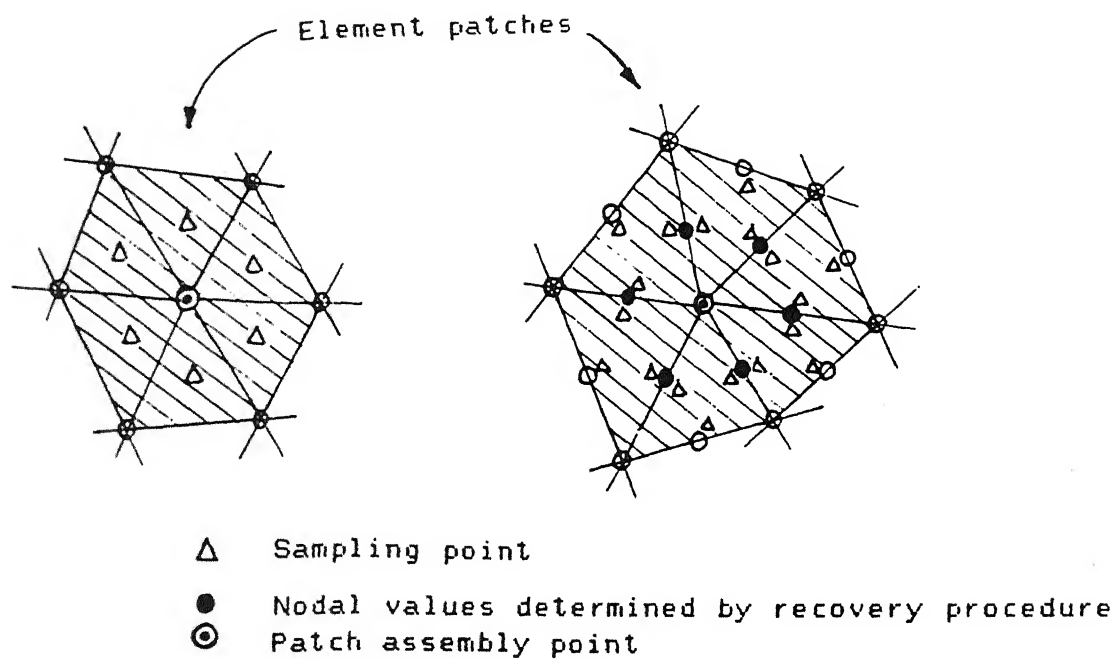


Figure 3.4 Computation of Superconvergent Nodal Values for Linear and Quadratic Triangular Elements

integration points.

In the linear form the average of the derivative values at mid sides of adjacent elements is proved to be superconvergent. For practical purposes, however, this is equivalent to stating that the centroidal point values of the element is superconvergent.

For quadratic triangles no fully superconvergent points appear to be known though it is suggested that some derivatives (those parallel to the sides) are superconvergent at two side Gauss points. Here, a simpler but purely experimental finding that the central values at sides are optimal, is used.

It is observed [Zienkiewicz et al., 1992] that element patches overlap for internal midside nodes and interior nodes in the element. This means that such recovered values are frequently evaluated from two patches. As all such values are superconvergent, an average value is used for such nodes. The recovered assembly (vertex) nodal values are, however, only determined from a single patch.

Thus, in this way the above formulation allows one to evaluate a posteriori errors of the finite element solution which is used to adaptively refine the existing mesh and thus a better approximation to the exact solution is obtained.

3.4 AUTOMATIC MESH REFINEMENT

Automatic mesh generation and refinement is an important part of adaptive mesh generation codes. The initial mesh generation, usually coarse mesh, can be quite simple in the case of simple domains such as rectangles, circles etc. or complex mapping techniques can be used in the case of irregular regions. In the present analysis rectangular plate bending problems are considered. A simple code was developed to divide the domain into triangular elements and output the nodal coordinates, connectivity etc. which is necessary for running the finite element analysis.

The mesh refinement part will be necessary while doing adaptive strategy and will be an integral part of the finite element analysis. When the error analysis is done and the element or elements to be subdivided are identified the code will appropriately modify the mesh and all the necessary information. The particular element may be refined by dividing it into two by creating an extra node at the centre of one of the edges and also subdividing the neighbouring element also as the elements have to be three noded triangles. Another way of subdividing can be making four smaller triangles of the original triangle to be subdivided by creating three nodes at the middle of the three edges and also subdividing the three neighbours (shown in Fig. 3.5) into two triangles each. Several other variations of subdividing the elements exist and in the present analysis the second procedure with further illustration in Fig. 3.6 is followed.

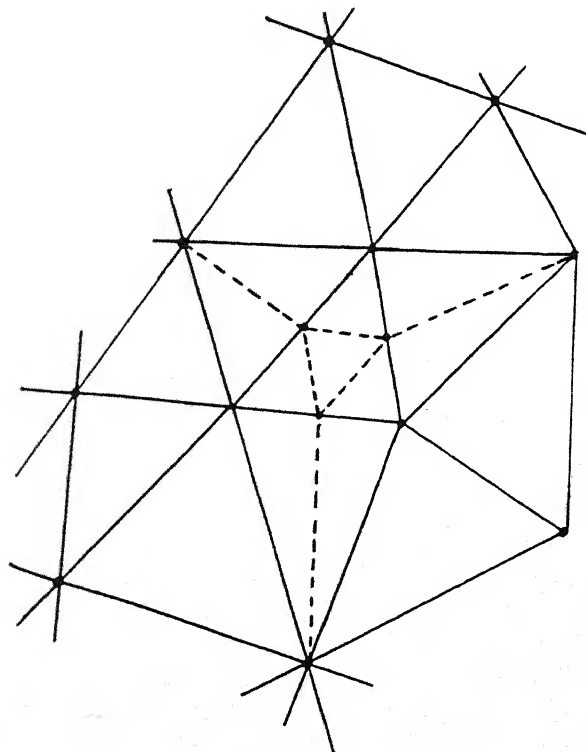
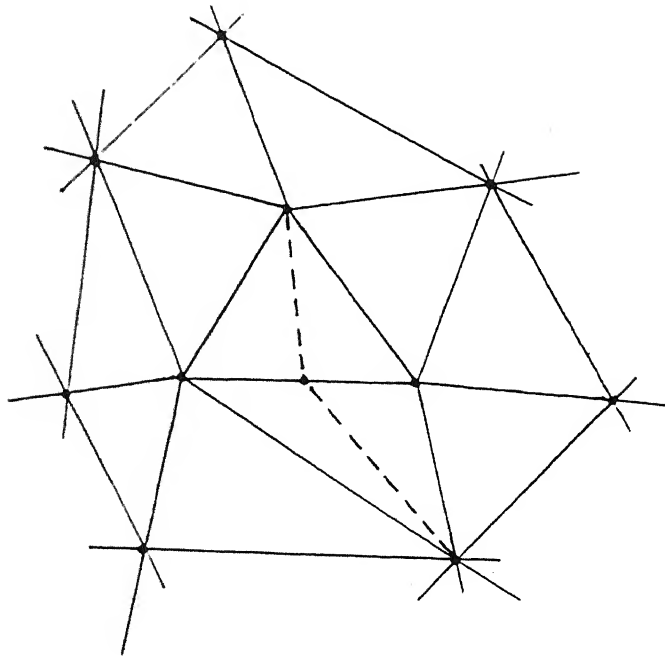


Figure 3.5 Some Element Subdivision Methods

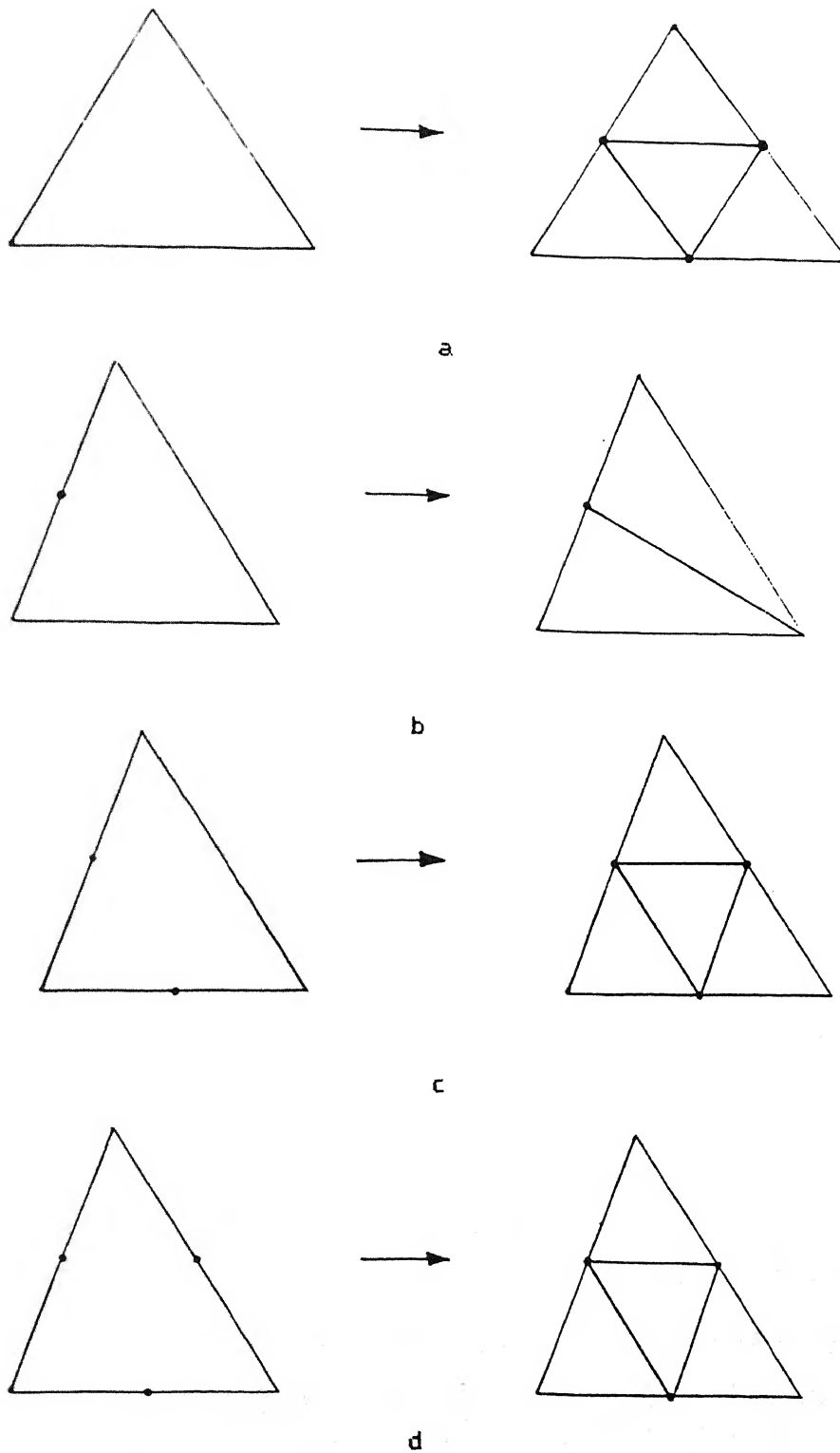


Figure 3.6 Element Subdivision Method Used in the Present Work

As can be seen these procedures require several neighbourhood arrays such as element-edges, edges-nodes, edges-elements etc. so as to identify and modify nodal array, element connectivity, nodal coordinates, boundary conditions etc.

After the mesh is refined and new nodes and elements created, the nodal locations are optimised so as to get better shape of triangles.

It is needless to say that the inclusion of graphic display of the mesh at various stages is a necessity in the development of the code.

3.5 ALGORITHM FOR ADAPTIVE MESH REFINEMENT

To implement the above the following algorithm is employed.

- (1) Divide the region into finite element mesh.
- (2) Obtain solution by finite element method and determine error norms in various elements. If the solution is satisfactory stop further refinement.
- (3) Decide the element to be subdivided.
- (4) Let k denote the triangle where the subdivision is to be done. This is divided into four smaller triangles, yielding new nodes at the mid points of the sides of the triangle in question (Fig. 3.6a). Triangles other than k but having new nodes on their sides are also divided (Fig. 3.6b-d). In this way mesh refinement proceeds iteratively. After each iteration mesh smoothing is done by adjusting the nodes such that each internal node lies at the

centrode of the polygon formed by the surrounding nodes.

$$x_i = \frac{1}{n} \sum_{l=1}^{n_i} x_l$$

$$y_i = \frac{1}{n} \sum_{l=1}^{n_i} y_l$$

where the summation is done over all nodes n_i surrounding the i th node. This helps in proper distribution of element sizes.

(5) Go back to (2).

CHAPTER IV

RESULTS AND DISCUSSION

This chapter describes the results of several problems illustrating the effectiveness of the adaptive finite element method presented in the previous chapters. The plate bending problem is solved starting with the triangular mesh configuration. After the first solution is obtained, a posteriori error estimates are made on different elements of the mesh. The errors on different elements are compared and the element having maximum error is subdivided. In fact it is a matter of convenience and suitability as to how many elements should be subdivided at each stage.

4.1 PLATE WITH NO CRACK

To validate the finite element code developed a square plate with all edges fixed and subject to uniformly distributed lateral load has been considered. The details of the plate are as given in Fig. 4.1a. Due to symmetry about the center lines only a quarter of the plate is considered to minimize computations (Fig. 4.1b).

This problem is solved with the starting mesh configuration shown in Fig. 4.2a. Adaptive mesh refinement is done to obtain better results. Values of lateral deflection w , and moments M_x , M_y along the central line parallel to the X-axis and the Y-axis are shown in Figs. 4.3 to Fig. 4.6. The analytical results are

also shown in the figure.

The errors are larger on the boundary of the plate where both the edges are fixed as is indicated in the symmetric quarter considered. Here in this case it is desirable to go for simultaneous subdivision of all the elements having energy norm error ratios (i.e. the ratio of energy norm error for an element with respect to the average of this error for all the elements) greater than one. This is followed in the present case. Since further iterations lead to large number of degrees of freedom the solutions for which can not be obtained by the computer system available, meshes only for three iterations have been shown (Fig. 4.2). It can be seen from the results that adaptively refined meshes give better approximation to the analytical values. The finite element results for maximum lateral deflection are within 3% error when compared with analytical results. Iterationwise errors with respect to the maximum lateral deflection are also given in Fig. 4.2.

4.2 PLATE WITH A CENTER CRACK

The problems related to cracks in a plate subjected to loading are important. As the stresses are very high near the crack tip (theoretically infinite), the element size and their distribution play an important role in the evaluation of stresses. The error determination and the consequent adaptive mesh generation play a crucial role in developing an efficient finite element code. In this context, a square plate with a center crack

is analyzed for various loading conditions.

EDGE MOMENTS :

In the case of a square plate carrying a center crack subjected to moments applied at the edges parallel to the crack such that the lateral deflection is zero at these edges and the other two edges of the plate are free, symmetry about the two center lines allows the plate to be analysed for the symmetric quarter (Figs. 4.7a and 4.7b). The starting mesh configuration for this case is shown in Fig. 4.8. The moment M_y values are plotted along the centre line parallel to the X-Axis. Also the theoretical values [Sih, 1977] near the crack tip are plotted (Fig. 4.9). The finite element values are seen to approximate the theoretical crack tip moment values within an error equal to 11.7 % for crack tip distance of 7.93 cm. With further iterations it can be inferred that the solution will become more accurate.

UNIFORMLY DISTRIBUTED LOADING :

Here in this case the plate has one pair of parallel edges fixed and the other two edges free. As in the earlier problem, this one also has symmetry about center lines and hence only a quarter plate is considered for finite element analysis (Figs 4.10a and 4.10b). The starting mesh configuration is shown in Fig. 4.11. Adaptive mesh refinement is carried out. It may be pointed out that in the present analysis the element having maximum error is subdivided adaptively though several elements can

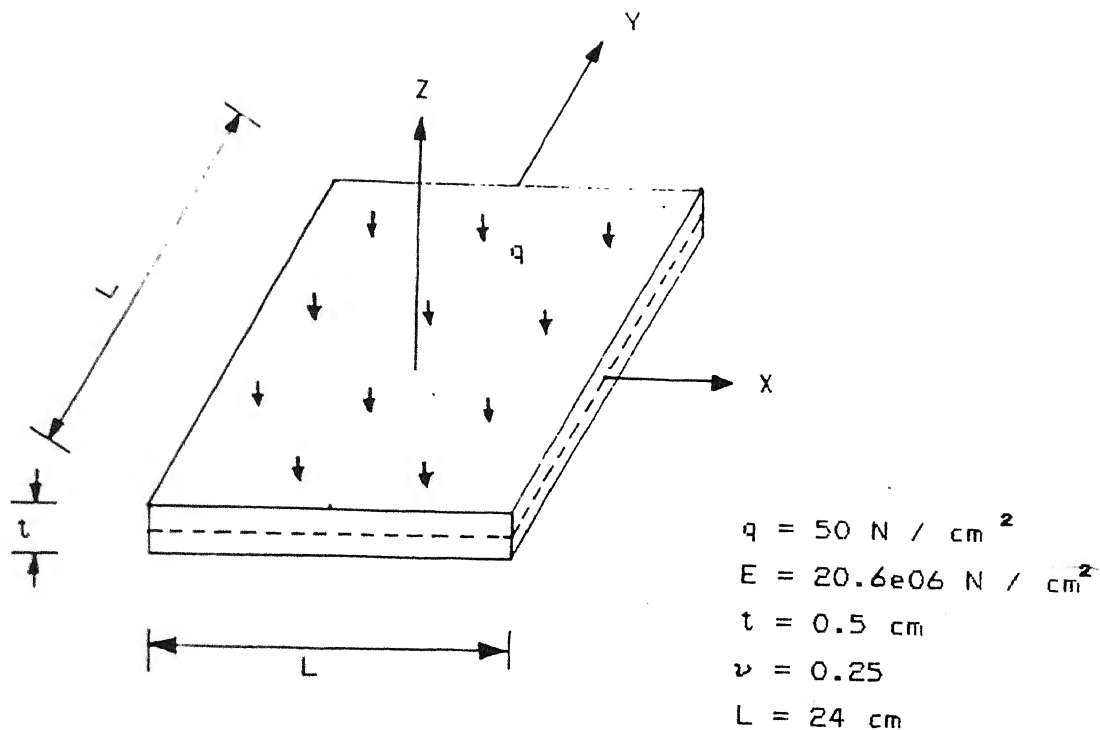


Figure 4.1a A Square Plate with all Edges Fixed and Subjected to Uniformly Distributed Lateral Loading

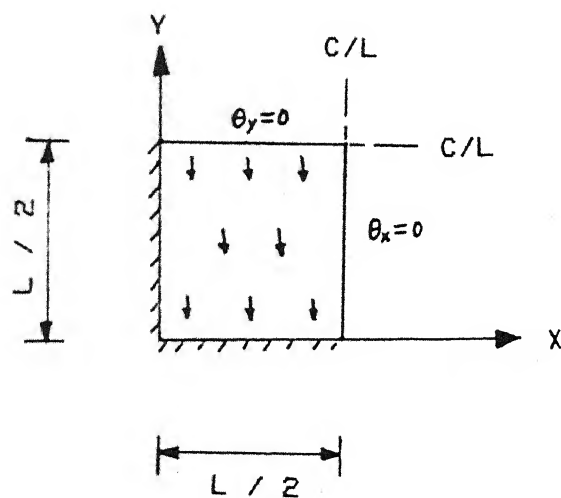
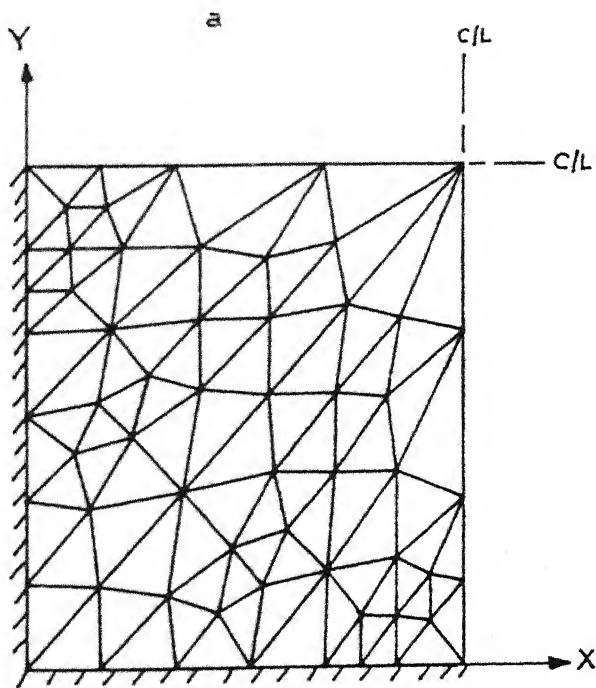
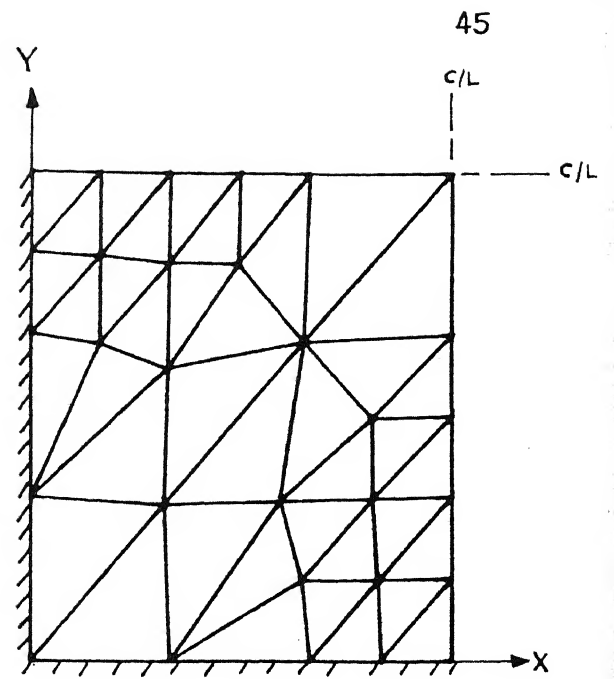
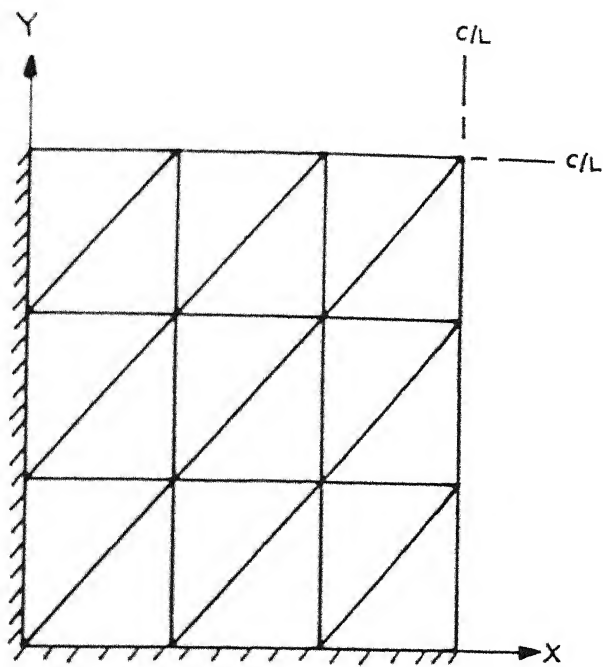


Figure 4.1b Symmetric Quarter of the Plate for the Case Shown in Fig. 4.1a



c

Figure 4.2 Mesh configurations at Different Stages of Adaptive Mesh Refinement for the Symmetric Quarter in Fig. 4.1b

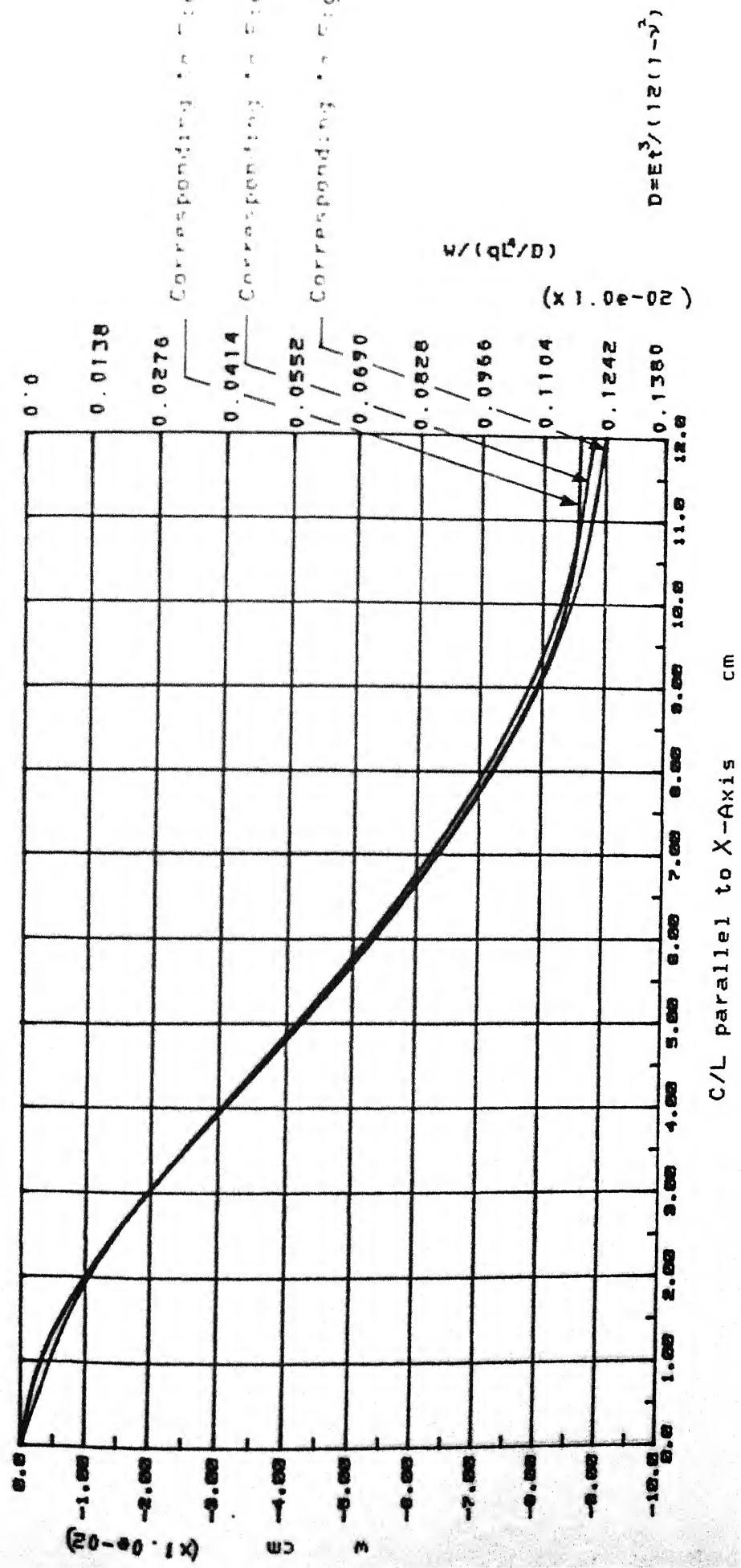
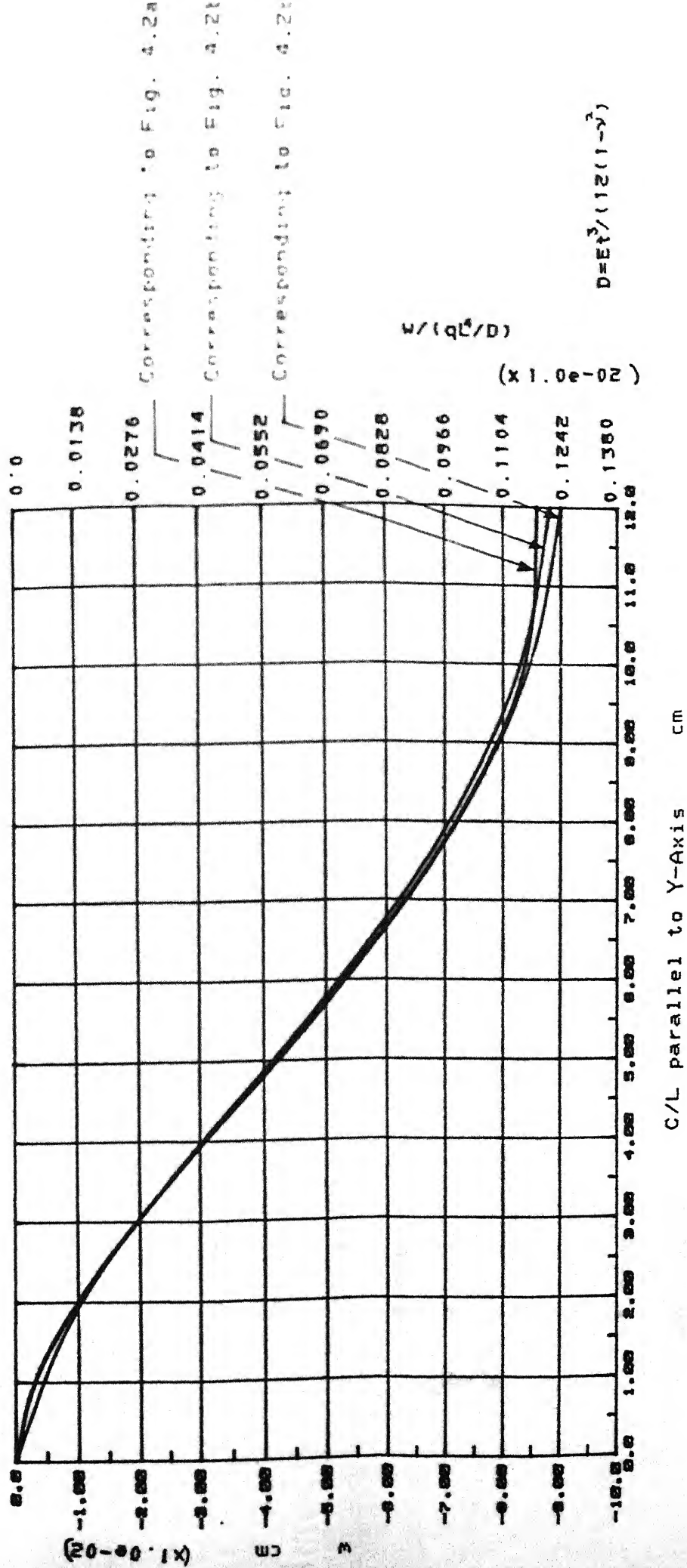


Figure 4.3 Variation of Lateral Displacement w along Center Line Parallel to X-Axis at Different Stages of Mesh Refinement for the Symmetric Quarter in Fig. 4.1b



Theoretical value of

max. lateral deflection = $9.13e-02$ cm

Iteration No.	% Error in max. lateral deflection
1	3.4 %
2	2.0 %
3	1.3 %

Figure 4.4 Variation of Lateral Displacement w along Center Line Parallel to Y-Axis at Different Stages of Mesh Refinement for the Symmetric Quarter in Fig. 4.1b

Corresponding to Fig. 4.2a

Corresponding to Fig. 4.2b

Corresponding to Fig. 4.2c

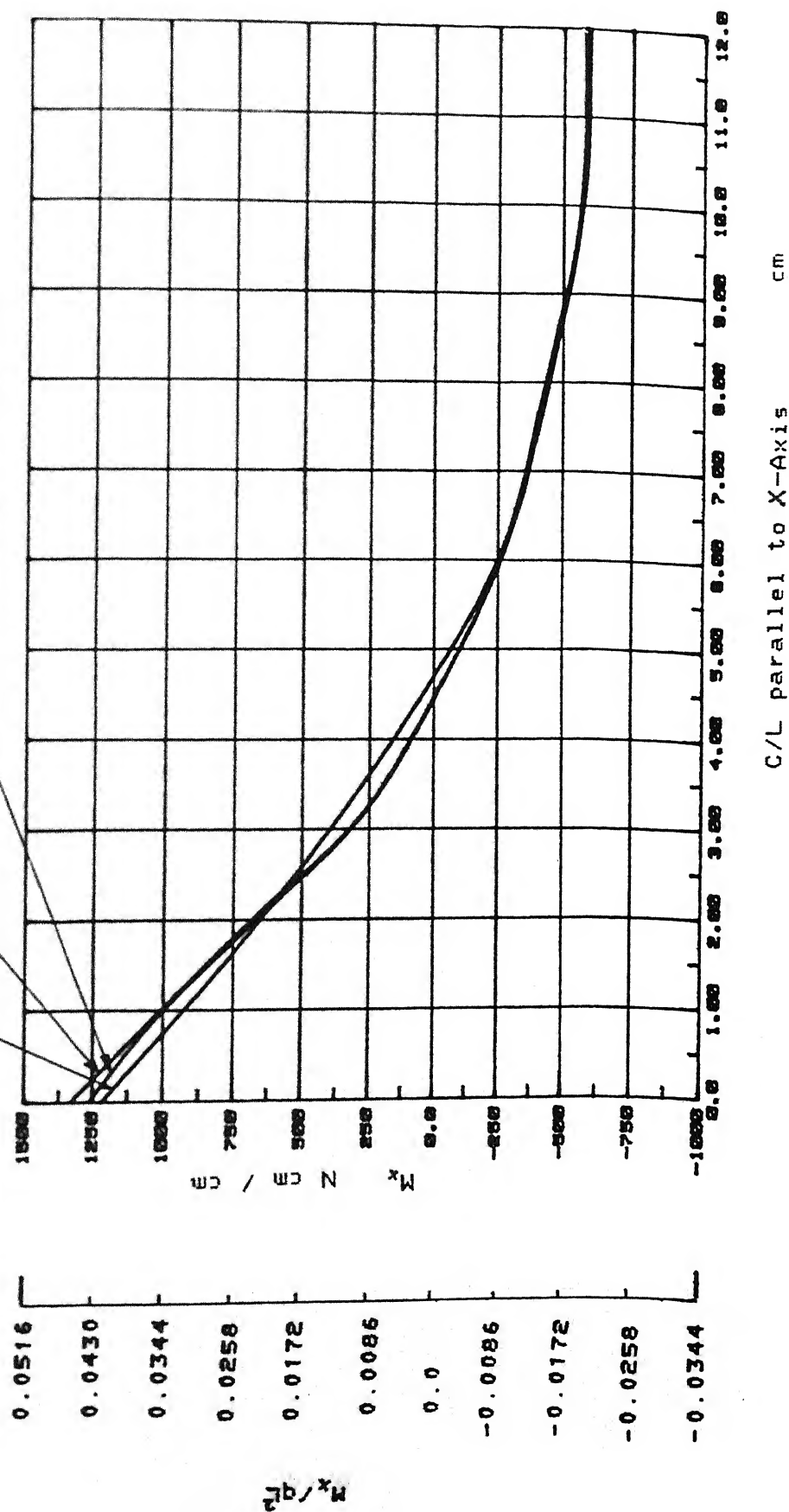


Figure 4.5 Variation of Moment, M_x along Center Line Parallel to X-Axis at Different Stages of Mesh Refinement for the Symmetric Quarter in Fig. 4.1b

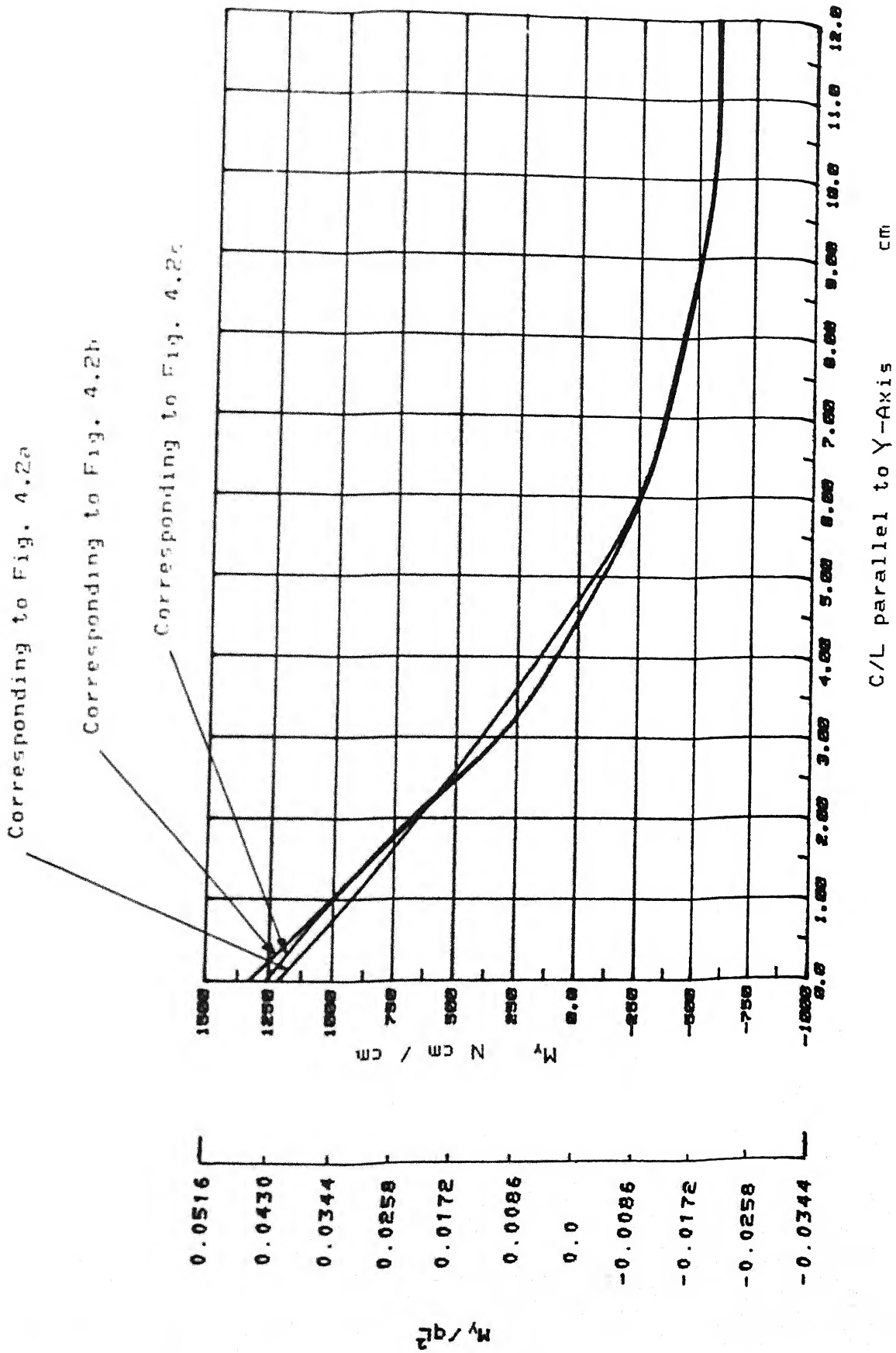


Figure 4.6 Variation of Moment, M_y along Center Line Parallel to Y-Axis at Different Stages of Mesh Refinement for the Symmetric Quarter in Fig. 4.1b

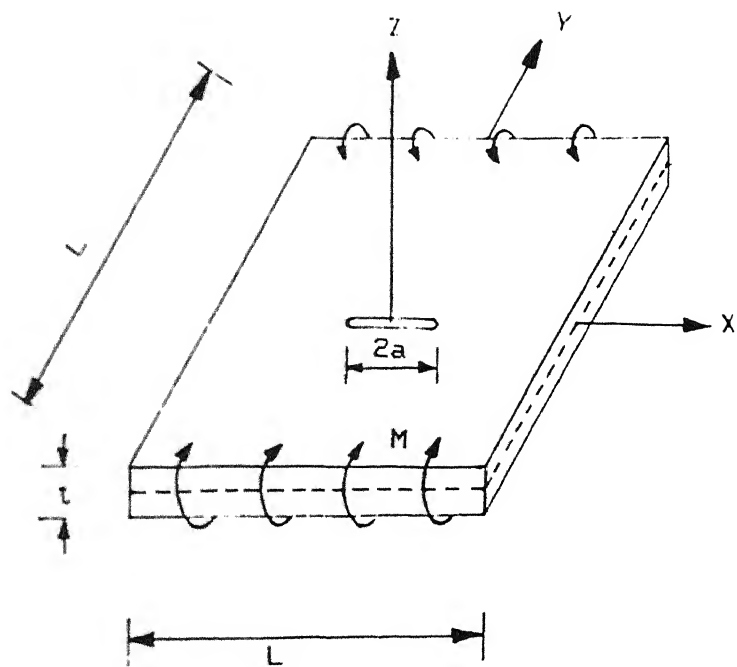


Figure 4.7 a A Square Plate with a Central Crack subjected to Uniformly Distributed Bending Moment at the Two Edges Parallel to the Crack and the Remaining Two Edges Free

$$\begin{aligned}
 M &= 70 \text{ N cm / cm} \\
 E &= 20.6 \text{e}06 \text{ N / cm}^2 \\
 t &= 0.5 \text{ cm} \\
 \nu &= 0.25 \\
 L &= 24 \text{ cm} \\
 a &= 4.0 \text{ cm}
 \end{aligned}$$

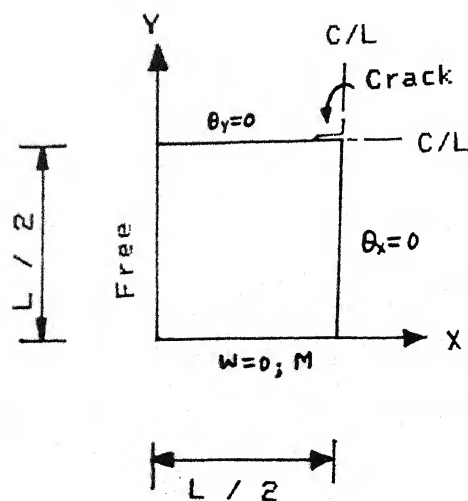


Figure 4.7 b Symmetric Quarter of the Plate for the Case Shown in Fig. 4.7a

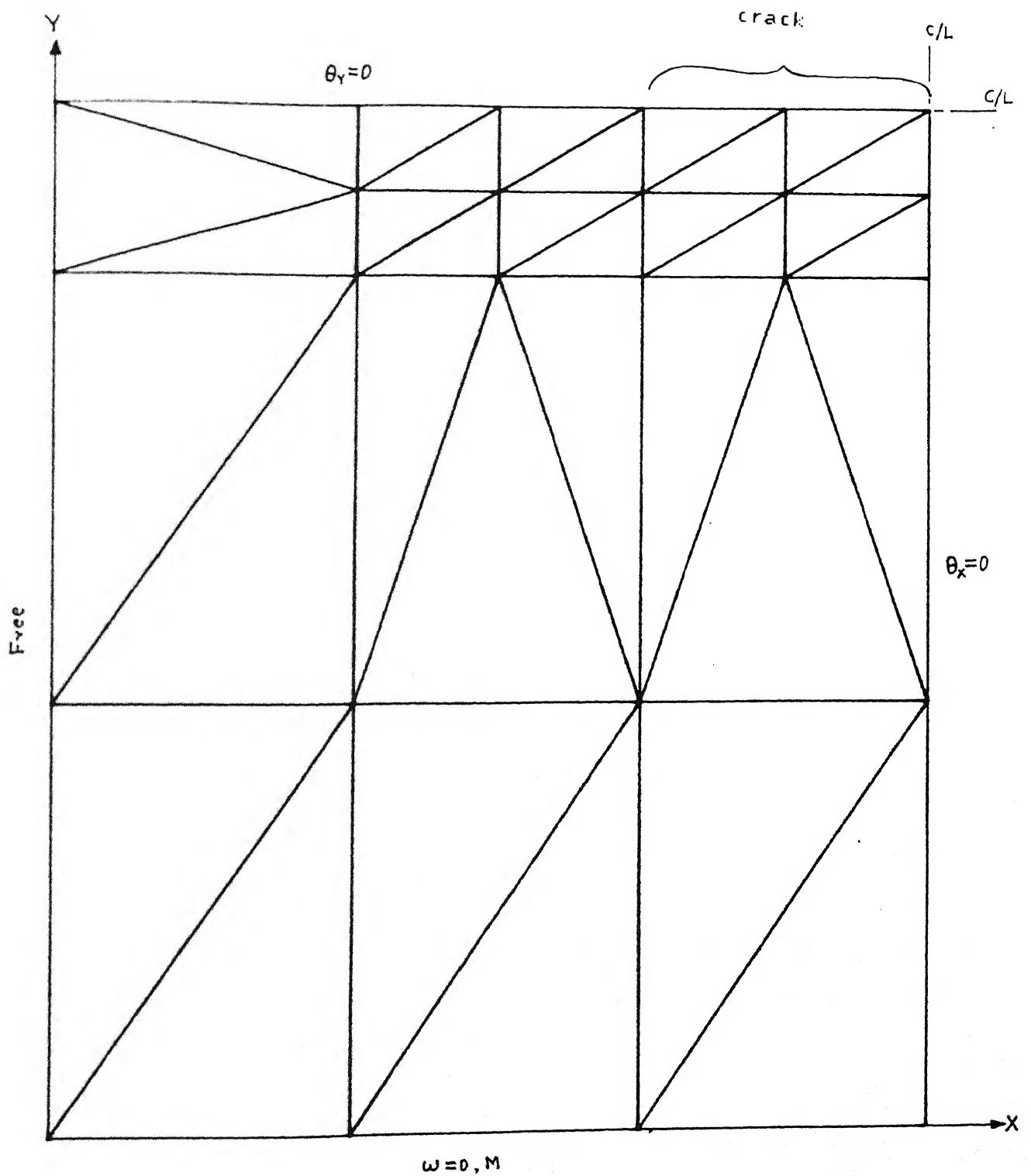


Figure 4.8

Starting Mesh Configuration for the Symmetric Quarter Shown in Fig. 4.7 b.

CENTRAL LIBRARY
I. I. T., KANPUR

Inv. No. A. 116268

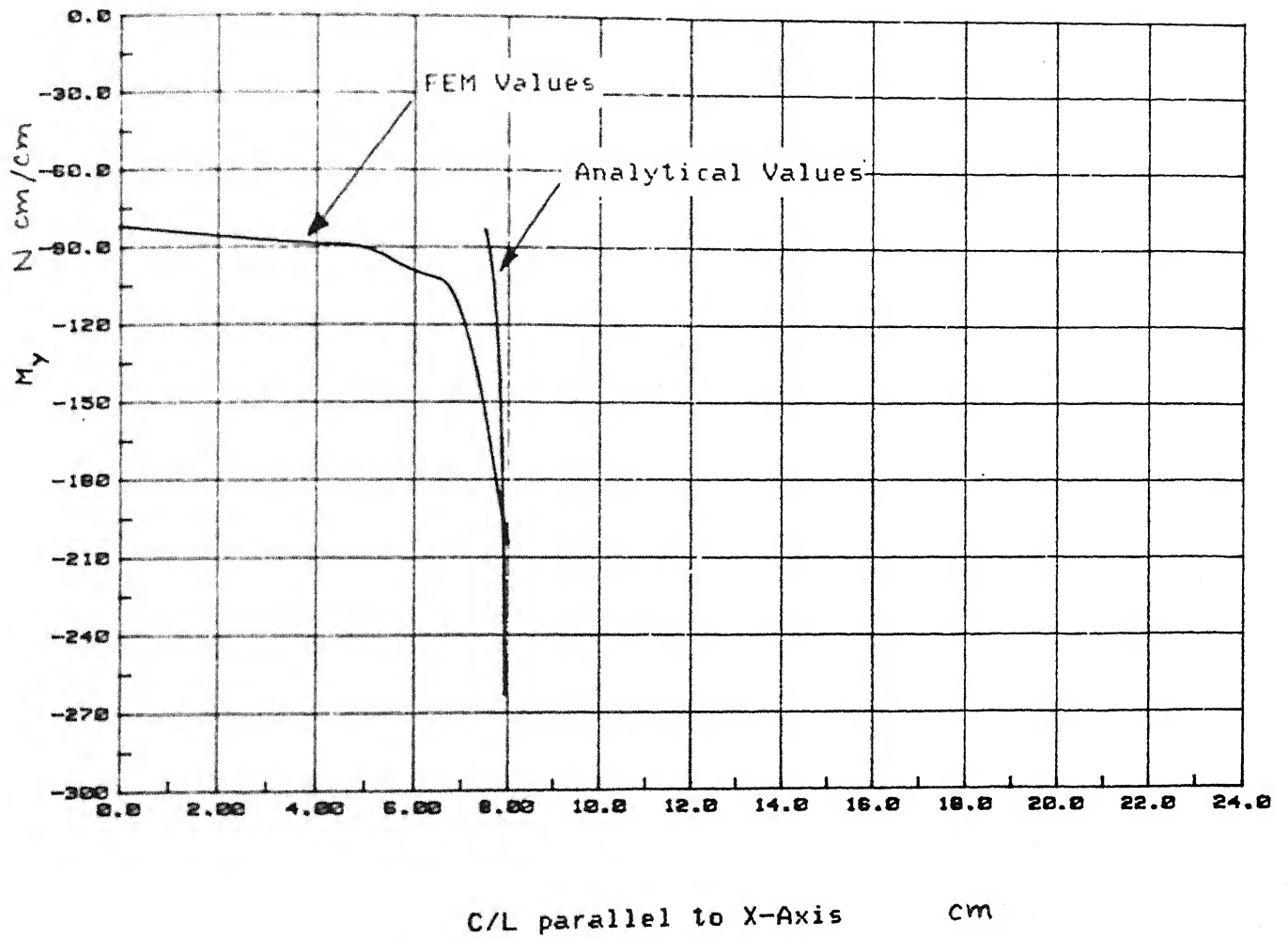


Figure 4.9 Variation of Moment M_y (FE Values and Analytical Values) along the Center Line Parallel to X-Axis for the Case Shown in Fig. 4.7b

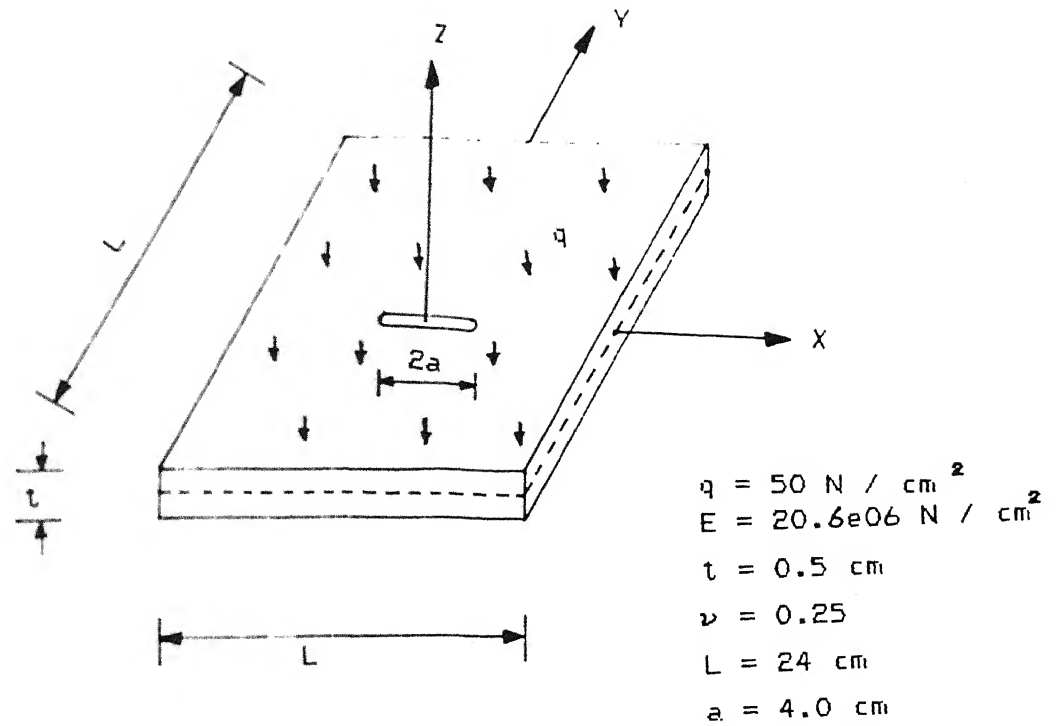


Fig. 4.10 a A Square Plate with a Central Crack Subjected to Uniformly Distributed Loading, two Edges Parallel to the Crack Fixed and the Remaining Two Edges Free

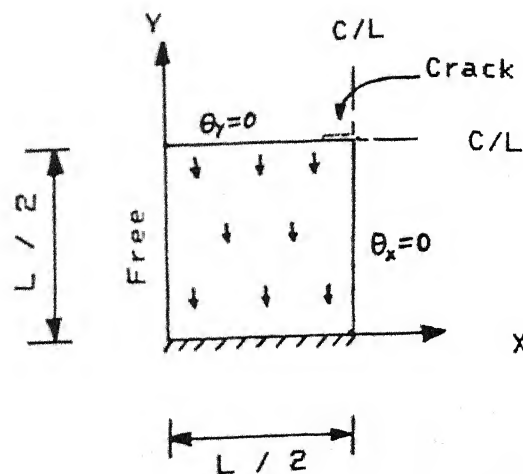


Figure 4.10 b Symmetric Quarter of the Plate for the Case Shown in Fig. 4.10a

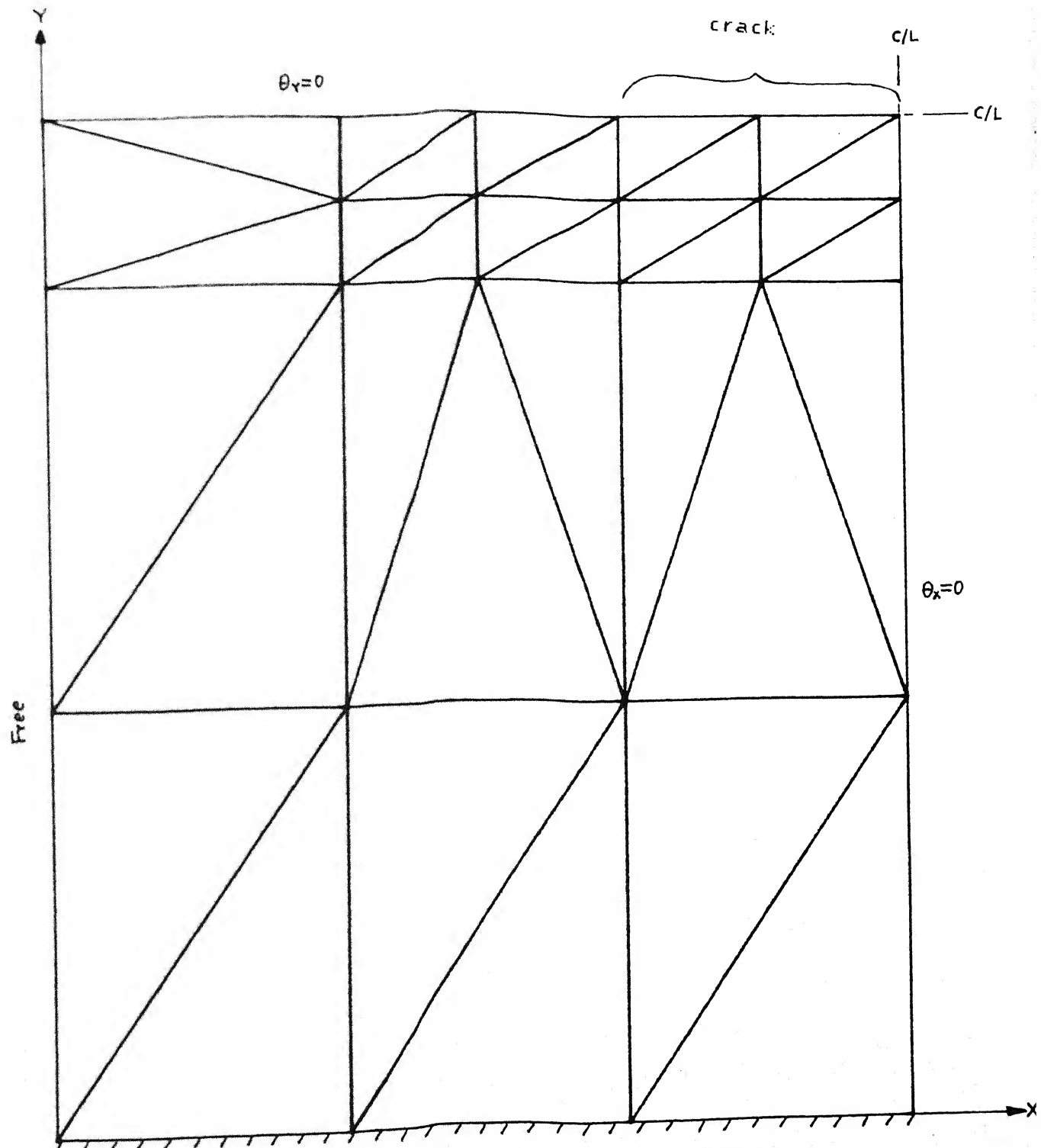


Figure 4.11 Starting Mesh Configuration for the Symmetric Quarter Shown in Fig. 4.10b

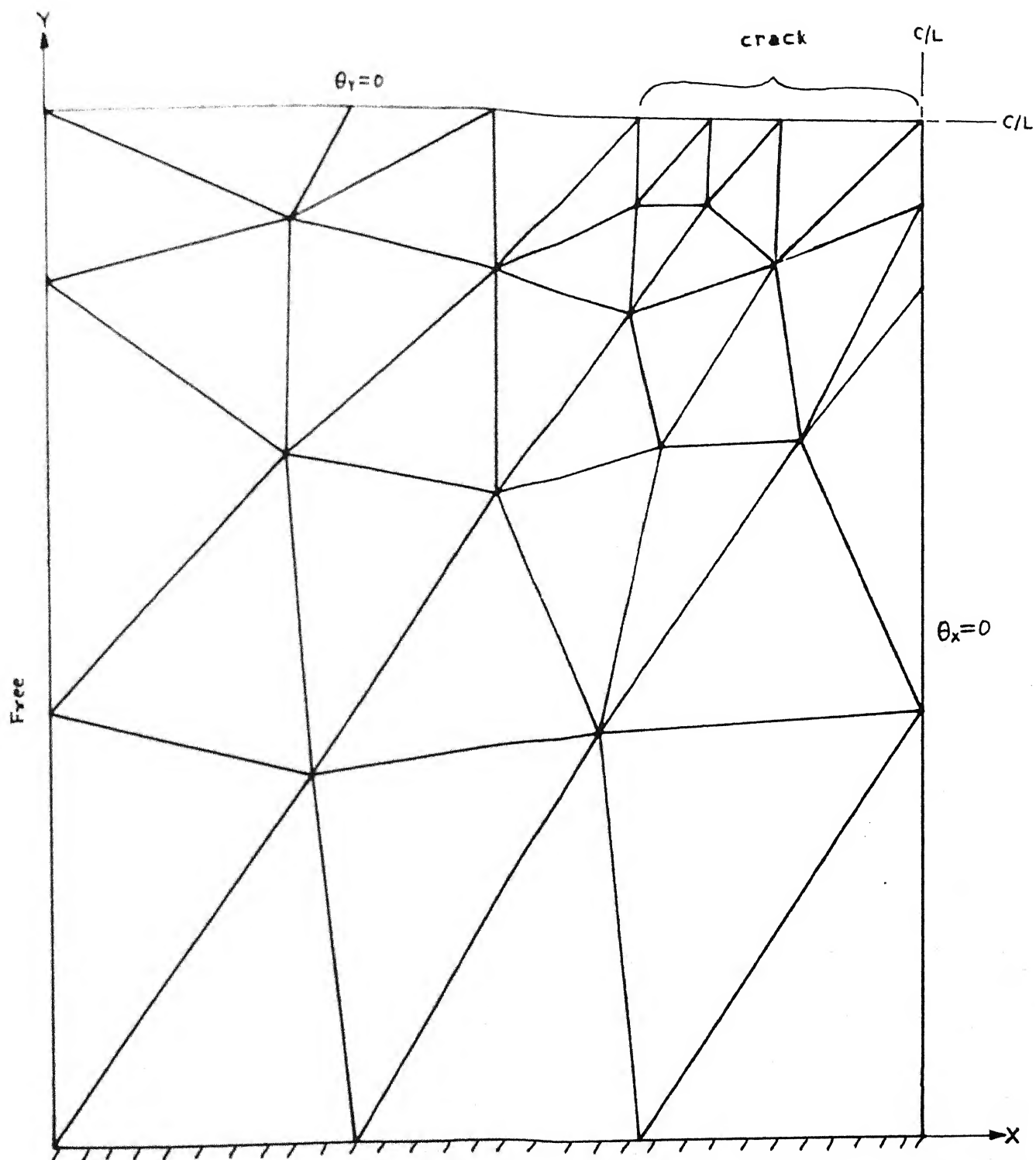


Figure 4.12a First Mesh Configuration

Figure 4.12

Mesh configurations at different stages of Adaptive Mesh Refinement for the Symmetric Quarter in Fig. 4.10.b

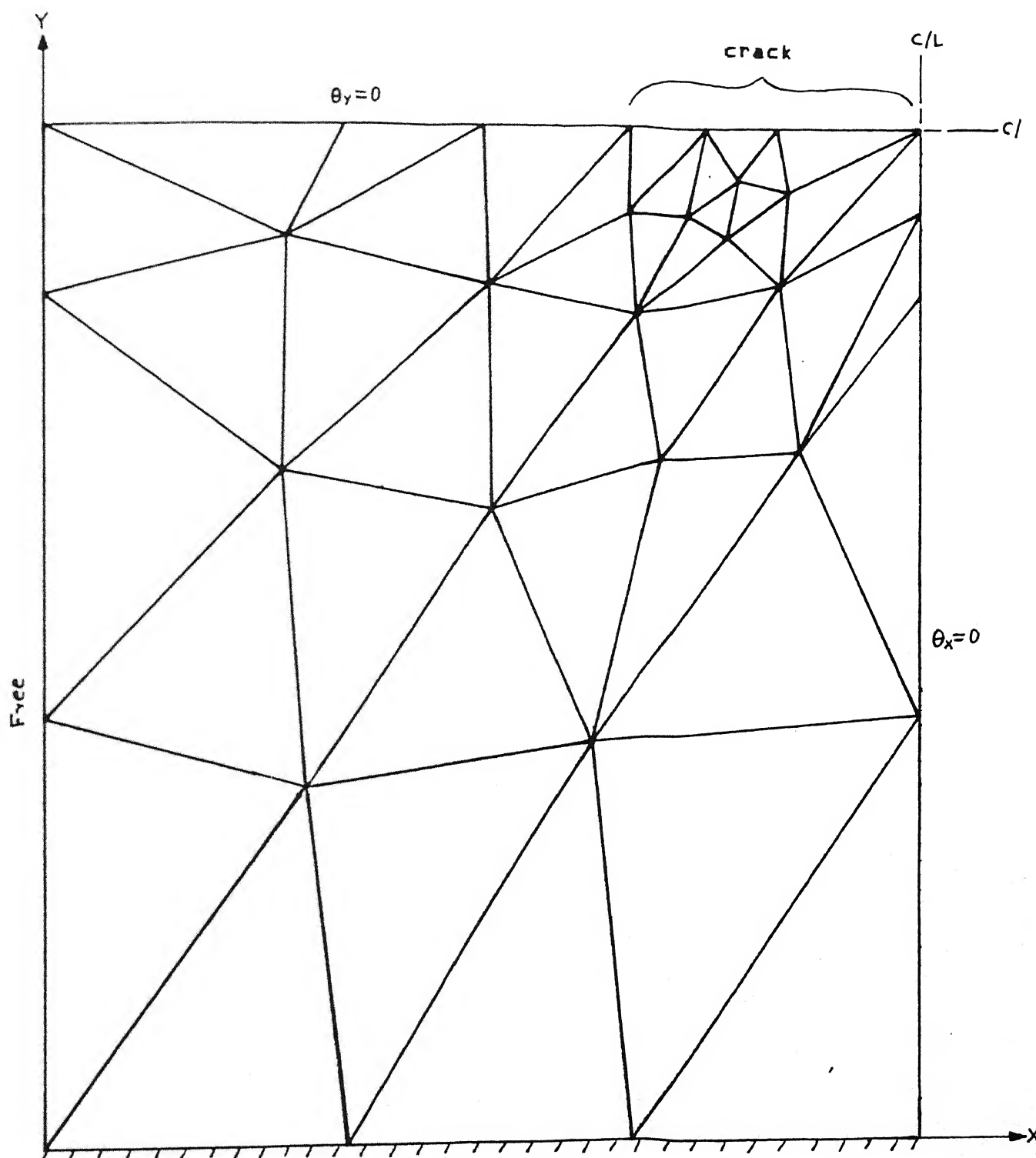


Figure 4.12b Second Mesh Configuration

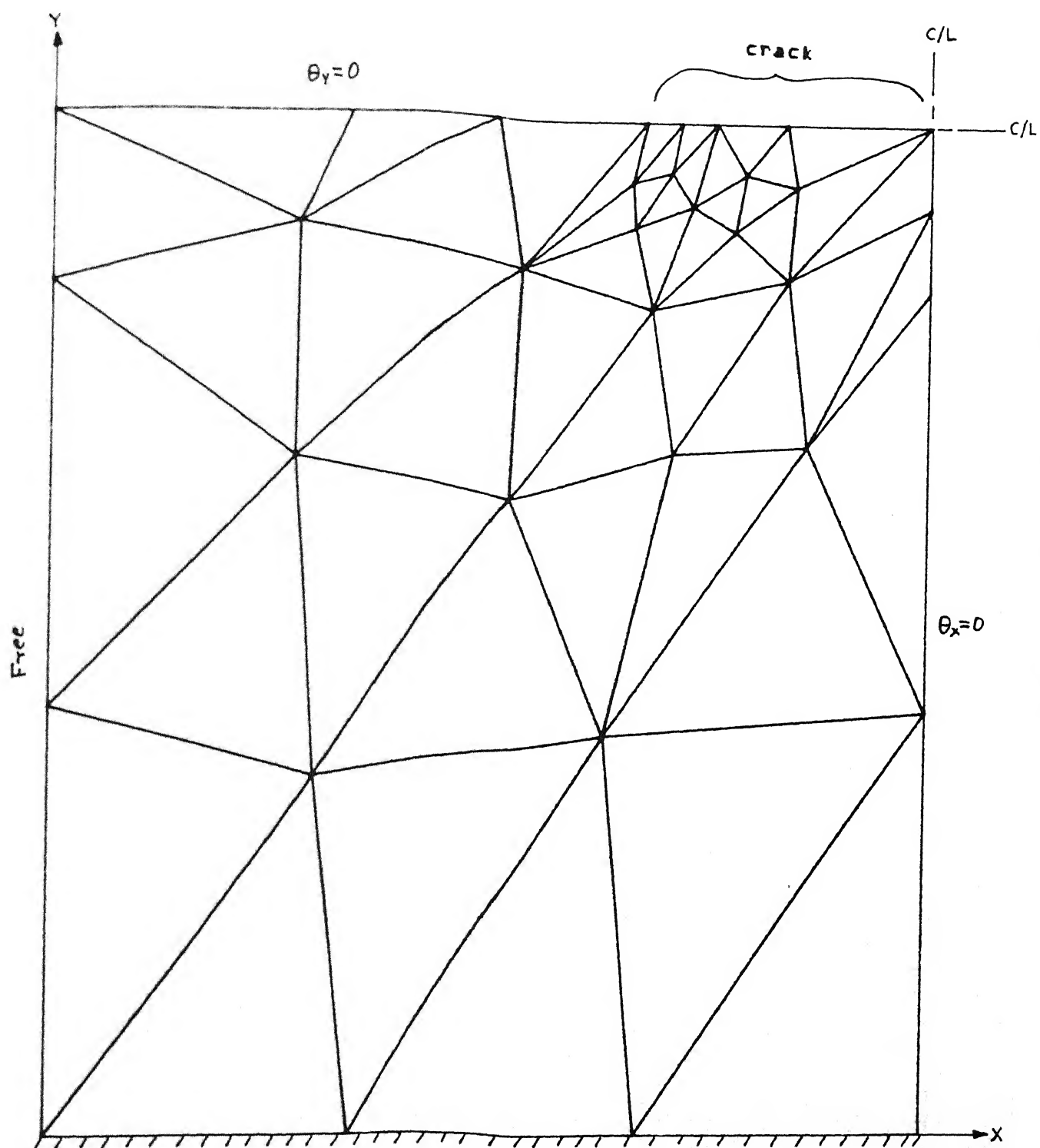


Figure 4.12c Third Mesh Configuration

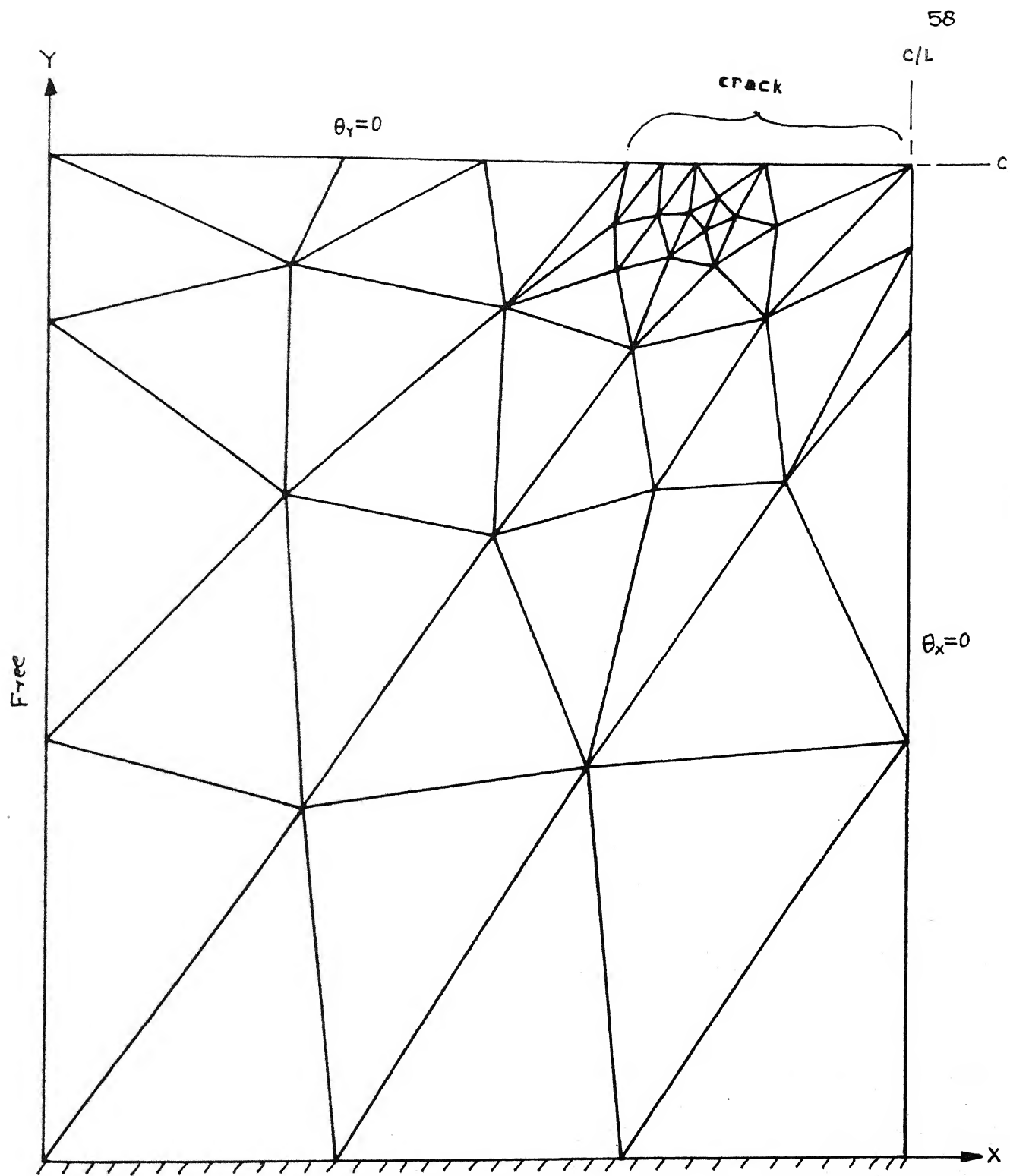


Figure 4.12d Fourth Mesh Configuration

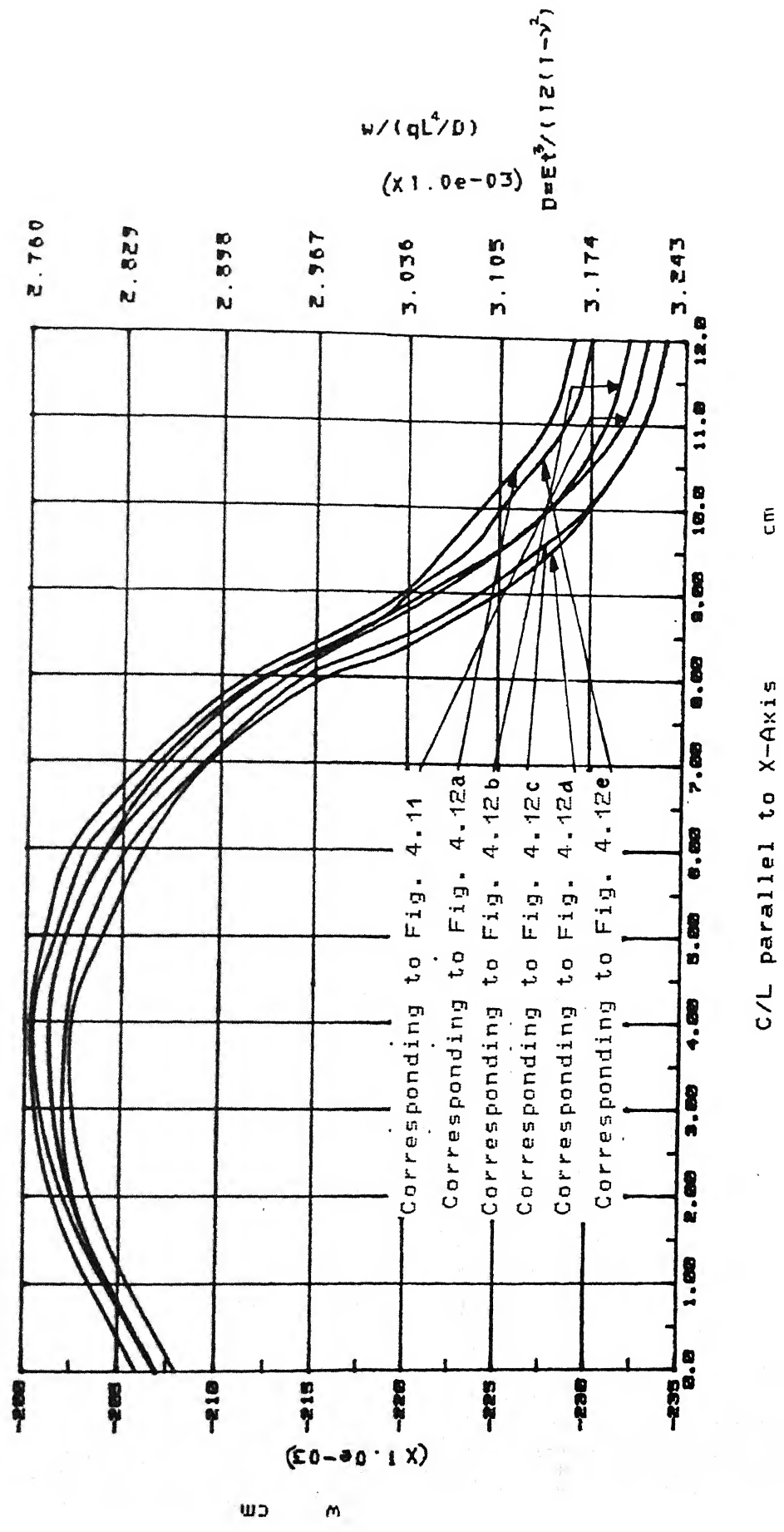


Figure 4.13 Variation of Lateral Displacement w along Center Line Parallel to X-Axis at Different Stages of Mesh Refinement for the Symmetric Quarter in Fig. 4.10b

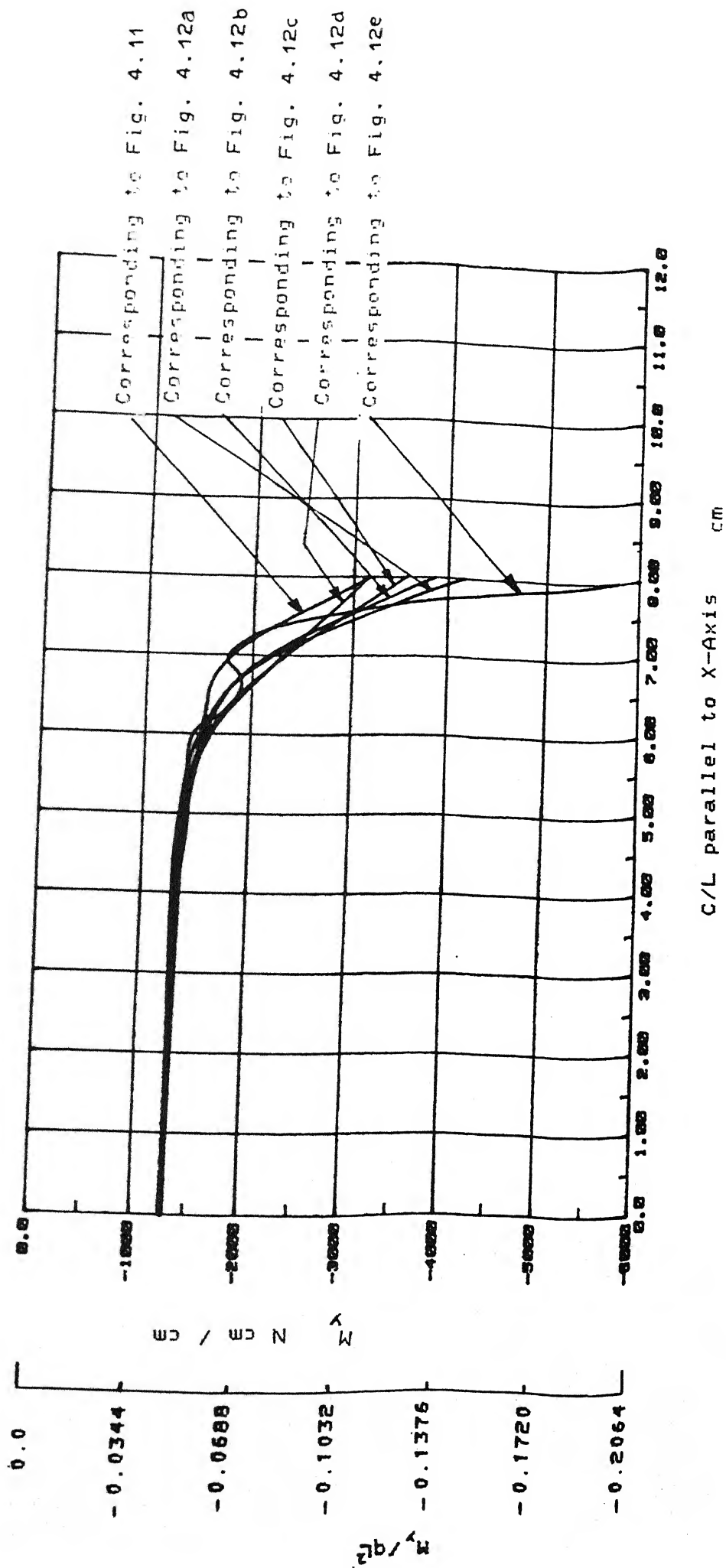


Figure 4.14 Variation of Moment M_y along Center Line Parallel to X-Axis at Different Stages of Mesh Refinement for the Symmetric Quarter in Fig. 4.10b

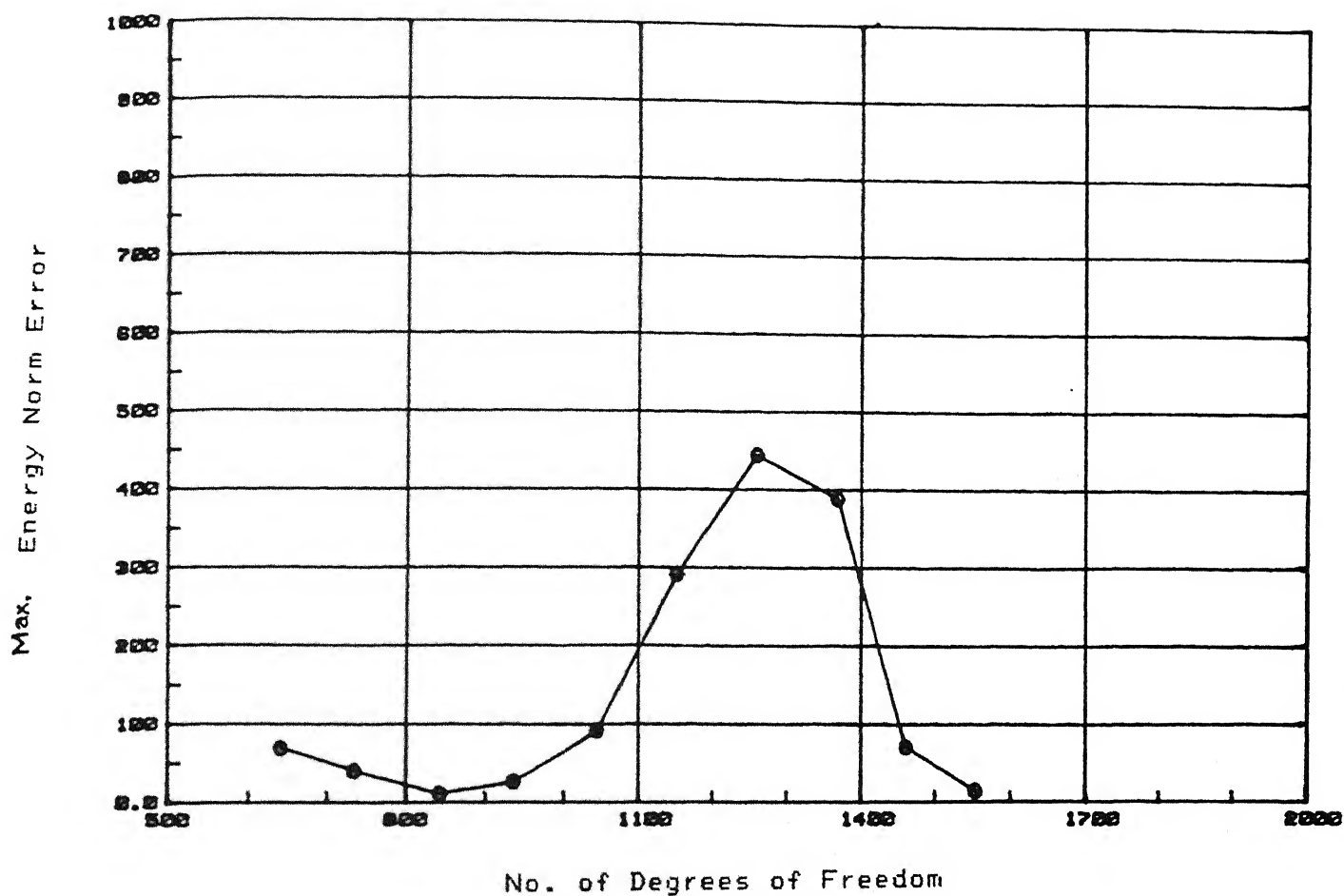


Figure 4.15 Variation of Maximum Energy Norm Error with Global Number of Degrees of Freedom for the Symmetric Quarter of the Plate Shown in Fig. 4.10b

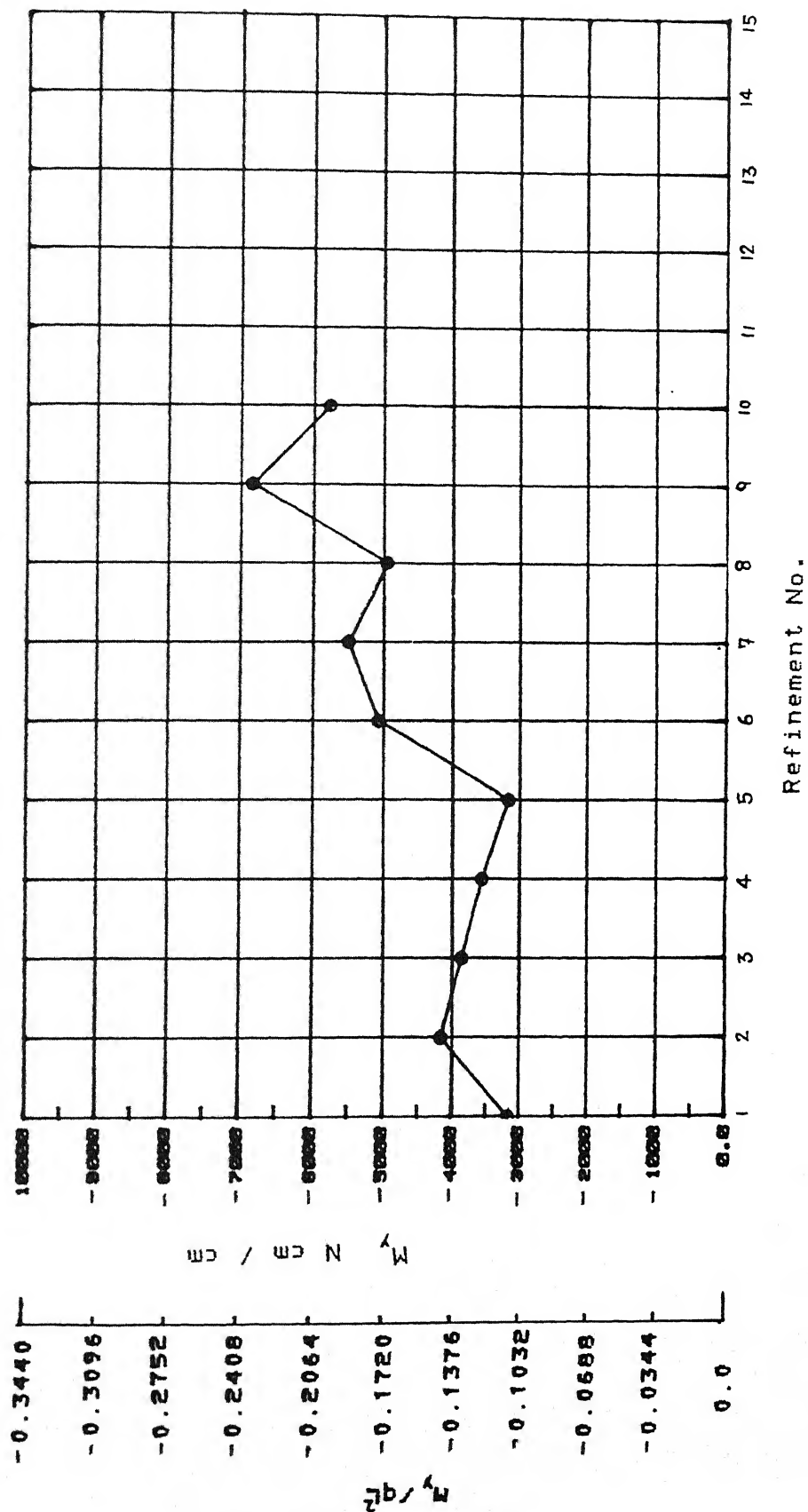


Figure 4.16 Variation of Crack Tip Moment M_y with respect to Different Stages of Mesh Refinement for Fig. 4.10 b

be subdivided at a time. This is done so as to observe the effectiveness of the adaptive strategy more clearly. It is seen that the elements near the crack tip are subdivided as the iteration proceeds. Five successive mesh configurations for the specified boundary conditions and subjected to a uniformly distributed load are shown in Figs. 4.12a to 4.12e. Fig. 4.12f gives mesh configuration for tenth refinement. The corresponding plots of lateral deflection w and moment M_y along the central line parallel to the X-axis are shown in Figs. 4.13 to 4.14.

It can be seen from the figures (Figs. 4.12a to 4.12f) that the mesh near the crack tip is adaptively getting refined finer and finer. This behaviour conforms to the expected one. The bending moment M_y when plotted along the center line parallel to the X-Axis can be seen to be increasing to a larger value near the crack tip. As the mesh is refined adaptively the crack tip value for M_y increases with some oscillatory behaviour. It is clear from the figure (Fig. 4.14) that the results of more and more refined meshes will lead to better results. The variation of the values of moment M_y at the crack tip with respect to different refinements when plotted (Fig. 4.16) shows the nature of its variation as refinement proceeds. It indicates that as the refinement is proceeding with smaller and smaller elements near the crack tip the value of M_y at the crack tip is increasing which is also desirable. Also the energy norm error when plotted against the number of degrees of freedom in different iterations (Fig.4.15) it is seen that it decreases to lower values as the

refinement proceeds though again some oscillations are present.

CHAPTER V

CONCLUSIONS AND SCOPE OF FURTHER WORK

5.1 CONCLUSIONS

Based on the adaptive finite element plate bending analyses for the cases without crack and with crack the following conclusions can be drawn

1. Based on the energy norm errors effective finite element mesh refinement techniques can be developed. Local superconvergent patch recovery techniques coupled with adaptive mesh refinement procedures allow for local mesh refinement.
2. As the mesh refinement proceeds the finite element results give better approximations to the solutions. Also it is observed that the maximum energy norm error decreases with some oscillations as the refinement process proceeds.

5.2 SCOPE OF FURTHER WORK

It was observed in the course of the present work that the element matrix gives very large number of global degrees of freedom. This makes the global stiffness matrix of a very high order (of the order of 1797×1797 with 96 elements). Handling such a large size matrix requires a lot of computer memory and budget. So element matrix condensation in the beginning will allow more refinement to be carried out. Another factor was the presence of zero diagonal elements in the element matrix. Development of a simultaneous equation solver which can take care

of such matrices as well as reduce the memory requirement for the storage can also be a further investigation.

REFERENCES

1. Ahamad, S., Irons B.M., Zienkiewicz, O.C., 'Curved thick shell and membrane elements with particular reference to axi-symmetric problems', Proc. 2nd conf. on matrix methods in standard mechanics, Wright Patterson Air Force Base, Ohio, 1968.
2. Ahamad, S., 'Curved finite element analysis of solid shell and plate structures', Ph.D. Thesis, University of Wales, Swansea, 1969.
3. Babuska, I., Rheinboldt, W.C., 'Error estimates for adaptive finite element computations', SIAM J. Num. Analysis, 15, (4), 1978.
4. Babuska, I., Rheinboldt, W.C., 'Adaptive approaches and reliability estimates in finite element analysis', Comp. Meth. Appl. Mech. Eng., 17/18, 519-540, 1979.
5. Babuska, I., Peano, Riccioni, R., Pasini, A., Sordella, L., 'Adaptive approximations in finite element structural analysis', ISMES, Bergamo, Italy, 1978.
6. Bathe, K.J., 'Finite Element Procedures in Engineering Analysis', Prentice Hall of India Pvt. Ltd., 1990.
7. Cook, R.D., 'Concepts and Applications of Finite Element Analysis, second edition, John Wiley & Sons, 1981.
8. Craig, A.W., Zhu, J.Z., Zienkiewicz, O.C., 'A posteriori error estimation, adaptive mesh refinement and multi-grid methods using hierarchical finite element bases', Whiteman, J.R., Mathematics of Finite Element Computations, Wiley, 1986.
9. Gago, J.P. De S.R., Kelly, D.W., Zienkiewicz, O.C., Babuska,

- I., 'A posteriori error analysis and adaptive processes in the finite element method: part II-adaptive mesh refinement', Int. j. numer. methods eng., 19, 1621-1656, 1983.
10. Hartranft, R.J., Sih, G.C., Journal of Mathematics and Physics, 47, 371-390, 1968..
11. Hinton, E., Salenen, E.M., Bicanic, N., 'A study of locking phenomena in isoparametric elements', in Whiteman, J.R.(ed), Mathematics of Finite Elements and Applications, MAFELAP 1978, Academic Press, 1979.
12. Jin, H., Wiberg, N.E., 'Two dimensional mesh generation, adaptive remeshing and refinement', Int. j. numer. methods eng., 29, 1501-1526, 1990.
13. Kelly, D.W., Gago, J.P. De S.R., Zienkiewicz, O.C., Babuska, I., 'A posteriori error analysis and adaptive processes in the finite element method: part I-error analysis', Int. j. numer. methods eng., 19, 1593-1619, 1983.
14. Knowles, J.K., Wang, N.M., Journal of Mathematics and Physics, 39, 223-236, 1960.
15. Lee, S.W., Wong, S.C., 'Mixed formulation finite element for Mindlin theory plate bending, Int. j. numer. methods eng., 18, 1297-1311, 1982.
16. Moan, T., 'Orthogonal polynomials and "best" numerical integration formulas on a triangle', ZAMM, 54, 501-508, 1974.
17. Murthy, M.V.V., Raju, K.W., Viswanath, S., 'On the bending stress distribution of a stationary crack from Riessner theory', Int. j. of fracture mechanics, 17, 6, 1981.
18. Pawsey, S.F., Clough, R.W., 'Improved numerical integration of

- thick slab finite elements', Int. j. numer. methods eng., 3, 575-586, 1971.
19. Pugh, E.D.L., Hinton, E., Zienkiewicz, O.C., 'A study of quadrilateral plate bending elements with reduced integration', Int. j. numer. methods eng., 12, 1059-1079, 1978.
20. Sih, G.C., 'Mechanics of Fracture', Vol. 3, 'Plates and Shells with Crack', Noordhoff International Publishing Leydon, 1977.
21. Timoshenko, S., Woinowsky-Krieger, S., 'Theory of Plates and Shells', McGraw Hill Book Company, Inc., 1959.
22. Wang, N.M., Journal of Mathematics and Physics, 47, 276-291, 1968.
23. Williams, M.L., Journal of Applied Mechanics, 24, 109-114, 1957.
24. Williams, M.L., Journal of Applied Mechanics, 28, 78-82, 1961.
25. Zienkiewicz, O.C., Taylor, R.L., 'The Finite Element Method', Fourth Edition, Vol. I, McGraw Hill Book Company, 1989.
26. Zienkiewicz, O.C., Taylor, R.L., 'The Finite Element Method', Fourth Edition, Vol. II, McGraw Hill Book Company, 1991.
27. Zienkiewicz, O.C., Too, J., Taylor, R.L., 'Reduced integration technique in general analysis of plates and shells', Int. j. numer. methods eng., 3, 275-290, 1971.
28. Zienkiewicz, O.C., Zhu, J.Z., 'A simple error estimator and adaptive procedure for practical engg. analysis', Int. j. numer. methods eng., 24, 337-357, 1987.
29. Zienkiewicz, O.C., Craig, A.W., 'A posteriori error estimation

and adaptive mesh refinement in finite element method', in Griffiths, David F. (ed) The Mathematical Basis of Finite Element Methods, Clarendon Press, Oxford, 1984.

30. Zienkiewicz, O.C., Lefebvre, D., 'A robust triangular plate bending element of the Reissner-Mindlin type, Int. j. numer. methods eng., 26, 1167-1184, 1988.

31. Zienkiewicz, O.C., Zhu, J.Z., 'Error estimator and adaptive refinement for plate bending problems', Int. j. numer. methods eng., 28, 2839-2853, 1989.

32. Zienkiewicz, O.C., Zhu, J.Z., 'The superconvergent patch recovery and a posteriori error estimates. Part I : the recovery technique', Int. j. numer. methods eng., 33, 1331-1364, 1992.

33. Zienkiewicz, O.C., Zhu, J.Z., 'The superconvergent patch recovery and a posteriori error estimates. Part II : error estimates and adaptivity', Int. j. numer. methods eng. 33, 1365-1382, 1992.